A discontinuous *hp* finite element method for convection–diffusion problems

Carlos Erik Baumann[1], J. Tinsley Oden*

Texas Institute for Computational and Applied Mathematics, The University of Texas at Austin, Austin, TX 78712, USA

Abstract

This paper presents a new method which exhibits the best features of both finite volume and finite element techniques. Special attention is given to the issues of conservation, flexible accuracy, and stability. The method is elementwise conservative, the order of polynomial approximation can be adjusted element by element, and the stability is *not* based on the introduction of artificial diffusion, but on the use of a very particular finite element formulation with discontinuous basis functions.

The method supports *h-*, *p-*, and *hp*-approximations and can be applied to any type of meshes, including non-matching grids. A priori error estimates and numerical experiments on representative model problems indicate that the method is robust and capable of delivering high accuracy. © 1999 Elsevier Science S.A. All rights reserved.

1. Introduction

We present the treatment of convection–diffusion problems using a new type of Galerkin method (DGM). In this method both the approximate solution and the associated fluxes can experience discontinuities across interelement boundaries. Among features of the method and aspects of the study presented here are the following:

- the method does not need auxiliary variables such as those used in hybrid or mixed methods;
- the method is robust and exhibits elementwise conservative approximations;
- the formulation is particularly convenient for time-dependent problems, because the global mass matrix is *block diagonal*, with *uncoupled* blocks;
- a priori error estimates are derived so that the parameters affecting the rate of convergence and limitations of the method are established;
- the method is suited for adaptive control of error, can deliver high-order accuracy where the solution is smooth; and
- the cost of solution and implementation is acceptable.

The solution of second-order partial differential equations with discontinuous basis functions dates back the the early 1970s, Nitsche [36] introduced the concept of replacing the Lagrange multipliers used in hybrid formulations with averaged normal fluxes at the boundaries, and added stabilization terms to produce optimal convergence rates. Similar approaches can be traced back to the work of Percell and Wheeler [39], and Arnold [3]. A different approach was the *p*-formulation of Delves and Hall [23], they developed the so-called Global Element Method (GEM); applications of the latter were presented by Hendry and Delves in [25]. The GEM

---

consists essentially in the classical hybrid formulation for a Poisson problem with the Lagrange multiplier eliminated in terms of the dependent variables; namely, the Lagrange multiplier is replaced by the average flux across interelement boundaries, without the addition of penalty terms. A major disadvantage of the GEM is that the matrix associated with space discretizations of diffusion operators is indefinite, therefore the method can not solve time dependent diffusion problems; and being indefinite, the linear systems associated with steady state problems needs special iterative schemes. The interior penalty formulations presented in [39] and [3] utilize the bilinear form of the GEM augmented with a penalty term which includes the jumps of the solution across elements. The disadvantages of the last approach include the dependence of stability and convergence rates on the penalty parameter, the loss of the conservation property at element level, and a bad conditioning of the matrices. The DGM for diffusion operators developed in this study is a modification of the GEM, which is free from the deficiencies mentioned earlier. More details on these formulations, and the relative merits of each one are presented in [10,38].

Among the applications of the Galerkin method to nonlinear first-order systems of equations, Cockburn and Shu [17–20] developed the TVB Runge–Kutta projection applied to general conservation laws; Allmaras [1] solved the Euler equations using piecewise constant and piecewise linear representations of the field variables; Lowrie [35] developed space–time discontinuous Galerkin methods for nonlinear acoustic waves; Bey and Oden [13] presented solutions to the Euler equations; Hu and Shu [26] presented solution to the Hamilton–Jacobi equations; and Atkins and Shu [4] presented a quadrature-free implementation for the Euler equations. Other applications of discontinuous Galerkin methods to first-order systems can be found in [14,28].

The solution of second-order systems of equations using discontinuous Galerkin approximations has been done mostly with mixed formulations, introducing auxiliary variables to cast the governing equations as a first-order system of equations. This methodology was used by Bassi and Rebay [9,8] for the solution of the Navier–Stokes equations, also Lomtev, Quillen and Karniadakis in [31–34] and Warburton et al. in [41] solved the Navier–Stokes equations discretizing the Euler fluxes with the DG method and using a mixed formulation for the viscous fluxes. A similar approach was followed by Cockburn and Shu in the development of the Local Discontinuous Galerkin method [21], see also a short-course notes by Cockburn [16]. Other methodologies which also used mixed approximations for the diffusion terms were developed by Dawson [22], and Arbogast and Wheeler [2]. The disadvantage of using mixed methods is that for a problem in $\mathbb{R}^d$, for each variable subject to a second-order differential operator, d more variables and equations have to be introduced to obtain a first-order system of equations.

In this paper we present a new method for the solution of convection–diffusion problems which is based on the classical discontinuous Galerkin approximation for convection terms [15,17,27,29,30] (summarized in Appendix A) and on the technique developed in [7,10,38] for diffusion terms. This new methodology supports h-, p-, and hp-version approximations and can produce highly accurate solutions. We explore the stability of the method and we present a priori error estimates.

Following this introduction, Section 2 presents the model problem, domain partitions and spaces of basis functions, Section 3 introduces the variational formulation, a stability study in special mesh-dependent norms and an a priori error estimate. Section 4 presents numerical experiments which confirm the theoretical results from Section 3 and applications which include the solution of the Euler and Navier–Stokes equations. Finally, conclusions are listed in Section 5 and Appendix A contains a review of the classical discontinuous Galerkin method for hyperbolic problems with a summary of a priori error estimates.

2. Governing equation and boundary conditions

We consider the following model problem: Let Ω be an open bounded Lipschitz domain in $\mathbb{R}^d$, such as the polygonal domain in $\mathbb{R}^2$ depicted in Fig. 1 and let us consider a model second-order convection–diffusion problem characterized by the following scalar partial differential equation

$$-\nabla \cdot (A\nabla u) + \nabla \cdot (\beta u) + \sigma u = S \quad \text{in } \Omega \subset \mathbb{R}^d \tag{7}$$
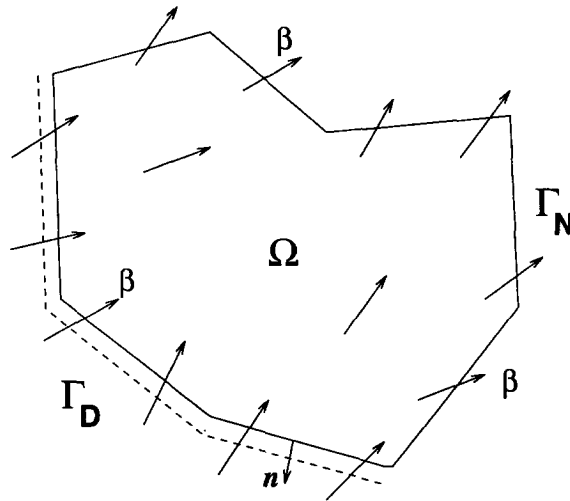
with boundary conditions

Fig. 1. Domain and boundaries—Notation.

$$\begin{array}{ll} u = f & \text{on } \Gamma_D \\ (A\nabla u) \cdot \boldsymbol{n} = g & \text{on } \Gamma_D \end{array} \tag{2}$$

where $\boldsymbol{\beta} \in (L^\infty(\Omega))^d$ is the mass flux vector which may have contact discontinuities, $\sigma \in L^\infty(\Omega)$, $\sigma > 0$ a.e. in Ω, $S \in L^2(\Omega)$, and $A \in (L^\infty(\Omega))^{d \times d}$ is a diffusivity matrix characterized as follows:

$$A(x) = A^{\mathrm{T}}(x), \tag{3}$$
$$\alpha_1 a^{\mathrm{T}} a \geqslant a^{\mathrm{T}} A(x) a \geqslant \alpha_0 a^{\mathrm{T}} a, \qquad \alpha_1 \geqslant \alpha_0 > 0, \quad \forall a \in \mathbb{R}^d,$$

a.e. in Ω.

The boundary $\partial\Omega$ consists of two disjoint parts, Γ_D on which Dirichlet conditions are imposed, and Γ_N on which Neumann conditions are imposed: $\Gamma_D \cap \Gamma_N = \emptyset$, $\Gamma_D \cup \Gamma_N = \partial\Omega$, and meas $\Gamma_D > 0$. We make the following assumption regarding the inflow part of the boundary Γ_-:

$$\Gamma_D \supseteq \Gamma_- = \{x \in \partial\Omega \mid \boldsymbol{\beta} \cdot \boldsymbol{n}(x) < 0 \text{ a.e.}\}.$$

2.1. Families of regular partitions

Since the discontinuous approximations are defined on partitions of the domain Ω, we now establish notations and conventions for families of regular partitions.

Let $\mathscr{P} = \{\mathscr{P}_h(\Omega)\}_{h>0}$ be a family of regular partitions of $\Omega \subset \mathbb{R}^d$ into $N \doteq N(\mathscr{P}_h)$ convex subdomains Ω_e, such that for $\mathscr{P}_h \in \mathscr{P}$,

$$\bar{\Omega} = \bigcup_{e=1}^{N(\mathscr{P}_h)} \bar{\Omega}_e, \quad \text{and} \quad \Omega_e \cap \Omega_f = \emptyset \quad \text{for } e \neq f. \tag{4}$$

The partitions $\mathscr{P}_h(\Omega)$ are regular in the sense that if $h_e = \text{diam}(\Omega_e)$, and $\rho_e = \sup\{\text{diam}(s) : \text{sphere } s \subset \Omega_e\}$, then for simplices

$$\frac{h_e}{\rho_e} \leqslant C \qquad 1 \leqslant e \leqslant N(\mathscr{P}_h), \tag{5}$$

for every $\mathscr{P}_h(\Omega)$, and for quadrilaterals/hexahedra, if $\hat{h}_e = \min\{$lengths of edges of $\partial\Omega_e\}$, $\alpha_e = \min\{$interior angles between intersecting edges/faces of $\partial\Omega_e\}$, then

$$\frac{h_e}{\hat{h}_e} \leqslant C, \qquad \cos(\alpha_e) < 1, \qquad 1 \leqslant e \leqslant N(\mathscr{P}_h), \tag{6}$$

for every $\mathscr{P}_h(\Omega)$.

Each subdomain Ω_e has a Lipschitzian boundary $\partial\Omega_e$, which consist of piecewise smooth arcs plus vertices for $d = 2$, and piecewise smooth surfaces and edges for $d = 3$.

Let us define the *interelement boundary* by

$$\Gamma_{\text{int}} = \bigcup_{\Omega_f, \Omega_e \in \mathscr{P}_h} (\partial\Omega_f \cap \partial\Omega_e). \tag{7}$$

On Γ_{int} we define $\boldsymbol{n} = \boldsymbol{n}_e$ on $(\partial\Omega_e \cap \partial\Omega_f) \subset \Gamma_{\text{int}}$ for indices e, f such that $e > f$.

2.2. Broken spaces

Let us define the so-called *broken spaces* on the partition $\mathscr{P}_h(\Omega)$:

$$H^m(\mathscr{P}_h) = \{v \in L^2(\Omega) : v|_{\Omega_e} \in H^m(\Omega) \ \forall \ \Omega_e \in \mathscr{P}_h(\Omega)\}, \tag{8}$$

if $v \in H^m(\Omega_e)$, the extension of v to the boundary $\partial\Omega_e$, indicated by the trace operation $\gamma_0 v$, is such that $\gamma_0 v \in H^{m-1/2}(\partial\Omega_e)$, $m > 1/2$. The trace of the normal derivative $\gamma_1 v \in H^{m-3/2}(\partial\Omega_e)$, $m > 3/2$, which will be written as $\nabla v \cdot \boldsymbol{n}|_{\partial\Omega_e}$, is interpreted as a generalized flux at the element boundary $\partial\Omega_e$.

With this notation, for $v|_{\Omega_e} \in H^{3/2+\epsilon}(\Omega_e)$ and $v|_{\Omega_f} \in H^{3/2+\epsilon}(\Omega_f)$, we introduce the *jump* operator [.] defined on $\Gamma_{ef} = \bar{\Omega}_e \cap \bar{\Omega}_f \neq \emptyset$ as follows:

$$[v] = (\gamma_0 v)|_{\partial\Omega_e \cap \Gamma_{ef}} - (\gamma_0 v)|_{\partial\Omega_f \cap \Gamma_{ef}}, \quad e > f, \tag{9}$$

and the *average* operator $\langle.\rangle$ for the normal flux is defined for $(A\nabla v) \cdot \boldsymbol{n} \in L^2(\Gamma_{ef})$, as

$$\langle (A\nabla v) \cdot \boldsymbol{n} \rangle = \frac{1}{2} (((A\nabla v) \cdot \boldsymbol{n})|_{\partial\Omega_e \cap \Gamma_{ef}} + ((A\nabla v) \cdot \boldsymbol{n})|_{\partial\Omega_f \cap \Gamma_{ef}}), \quad e > f, \tag{10}$$

where A is the diffusivity matrix. Note that $\boldsymbol{n}$ represents the outward normal from the element with higher index.

3. The discontinuous Galerkin method

The aim of this paper is to present a discontinuous Galerkin formulation for convection–diffusion problems. Given that the formulation to be presented is built as an extension of the classical discontinuous Galerkin method for hyperbolic problems [15,17,27,29], we assume that the reader is familiar with the notation and formulations presented in Appendix A.

3.1. Weak formulation

Let $W(\mathscr{P}_h)$ be the Hilbert space on the partition $\mathscr{P}_h$ defined as the completion of $H^{3/2+\epsilon}(\mathscr{P}_h)$ under the norm $\|.\|_W$ defined as follows (induced by (16))

$$\|u\|_W^2 = \|u\|_V^2 + \|u\|_\beta^2 + \|u\sigma^{1/2}\|_{0,\Omega}^2, \tag{11}$$

$$\|v\|_V^2 = \sum_{\Omega_e \in \mathscr{P}_h} \int_{\Omega_e} \nabla v \cdot A\nabla v \, \mathrm{d}x + |v|_{0,\Gamma_{\mathscr{P}_h}}^2, \tag{12}$$

$$\|u\|_\beta^2 = |u|\beta|^{1/2}|_{0,\Omega}^2 + \sum_{\Omega_e \in \mathscr{P}_h} |\nabla u \cdot \beta/|\beta|^{1/2}|_{0,\Omega_e}^2 + |u|\beta \cdot n|^{1/2}|_{0,\Gamma_+}^2$$
$$+ |h^\alpha u^-|\beta \cdot n|^{1/2}|_{0,\Gamma_{\text{int}}}^2 + |h^{-\alpha}[u]|\beta \cdot n|^{1/2}|_{0,\Gamma_{\text{int}}}^2 , \tag{13}$$

$$|v|_{0,\Gamma_{\mathscr{P}_h}}^2 = |h^{-\alpha}v|_{0,\Gamma_{\text{D}}}^2 + |h^\alpha(A\nabla v) \cdot n|_{0,\Gamma_{\text{D}}}^2 + |h^{-\alpha}[v]|_{0,\Gamma_{\text{int}}}^2 + |h^\alpha\langle(A\nabla v) \cdot n\rangle|_{0,\Gamma_{\text{min}}}^2 , \tag{14}$$

and

$$|v|_{0,\Gamma}^2 = \int_\Gamma v^2 \, \mathrm{d}s , \quad \text{for } \Gamma \in \{\Gamma_{\text{D}}, \Gamma_{\text{N}}, \Gamma_{\text{int}}\} .$$

The terms $h^{\pm\alpha}$, with $\alpha = 1/2$, are introduced to minimize the mesh-dependence of an otherwise strongly mesh-dependent norm. In (14), the value of h is $h_e/(2\alpha_1)$ on Γ_{D}, and the average $(h_e + h_f)/(2\alpha_1)$ on that part of Γ_{int} shared by two generic elements Ω_e and Ω_f, the constant α_1 was defined in (3). In (13), however, h is $h_e/2$ on Γ_{D}, and the average $(h_e + h_f)/2$ on $\partial\Omega_e \cap \partial\Omega_f$.

A consistent formulation of problem (1)–(2) is the following variational statement:

> Find $u \in W(\mathscr{P}_h)$ such that
>
> $B(u, v) = L(v) \quad \forall v \in W(\mathscr{P}_h)$

(15)

where

$$B(u, v) = \sum_{\Omega_e \in \mathscr{P}_h} \left\{ \int_{\Omega_e} [\nabla v \cdot A\nabla u - (\nabla v \cdot \beta)u + v\sigma u] \, \mathrm{d}x \right.$$
$$\left. + \int_{\partial\Omega_e \backslash \Gamma_-} vu^-(\beta \cdot n_e) \, \mathrm{d}s \right\} + \int_{\Gamma_{\text{D}}} ((A\nabla v) \cdot nu - v(A\nabla u) \cdot n) \, \mathrm{d}s$$
$$+ \int_{\Gamma_{\text{int}}} (\langle(A\nabla v) \cdot n\rangle[u] - \langle(A\nabla u) \cdot n\rangle[v]) \, \mathrm{d}s ,$$
$$u^\pm = \lim_{\epsilon \to 0} u(x \pm \epsilon\beta) , \quad \text{for } x \in \Gamma_{\text{int}} , \tag{16}$$

see Fig. A.1 in Appendix A, and

$$L(v) = \sum_{\Omega_e \in \mathscr{P}_h} \int_{\Omega_e} vS \, \mathrm{d}x + \int_{\Gamma_{\text{D}}} (A\nabla v) \cdot nf \, \mathrm{d}s + \int_{\Gamma_{\text{N}}} vg \, \mathrm{d}s - \int_{\Gamma_-} vf(\beta \cdot n) \, \mathrm{d}s . \tag{17}$$

REMARK. The space $H_0^1(\Omega) \subset W(\mathscr{P}_h)$, and for $u, v \in H_0^1(\Omega)$ the bilinear and linear forms $B(u, v)$ and $L(v)$ reduce to those of the continuous Galerkin formulation, which is known to be unstable for convection–diffusion problems. The use of discontinuous basis functions in combination with (16)–(17), however, produces a method with superior stability properties.

3.2. Conservation property

In this section, we prove that the formulation presented is globally and locally conservative. Using the unity weight function $\forall \, \Omega_e \in \mathscr{P}_h(\Omega)$ in (15), we obtain

$$\int_{\Gamma_+} (\beta \cdot n)u \, \mathrm{d}s + \int_{\Gamma_-} f(\beta \cdot n) \, \mathrm{d}s - \int_{\Gamma_{\text{N}}} g \, \mathrm{d}s - \int_{\Gamma_{\text{D}}} (A\nabla u) \cdot n \, \mathrm{d}s = \sum_{\Omega_e \in \mathscr{P}_h} \int_{\Omega_e} (S - \sigma u) \, \mathrm{d}x ,$$

which is the expression of conservation at global level.

If we now use a weight function which is unity on a generic element Ω_e, and zero at any other element, from (15) we obtain

$$\int_{\partial\Omega_e\cap\Gamma_+} (\boldsymbol{\beta}\cdot\boldsymbol{n})u\,\mathrm{d}s + \int_{\partial\Omega_e\cap\Gamma_-} f(\boldsymbol{\beta}\cdot\boldsymbol{n})\,\mathrm{d}s - \int_{\partial\Omega_e\cap\Gamma_\mathrm{N}} g\,\mathrm{d}s - \int_{\partial\Omega_e\cap\Gamma_\mathrm{D}} (A\nabla u)\cdot\boldsymbol{n}\,\mathrm{d}s$$

$$+ \int_{\partial\Omega_e\cap\Gamma_\mathrm{int}} ((\boldsymbol{\beta}\cdot\boldsymbol{n}_e)u^- - \langle(A\nabla u)\cdot\boldsymbol{n}_e\rangle)\,\mathrm{d}s = \int_{\Omega_e} (S - \sigma u)\,\mathrm{d}\boldsymbol{x}\,,$$

which is the expression of conservation at element level.

3.3. Existence and stability of solutions

The existence of solutions to (15) can be established using the classical Generalized Lax–Milgram theorem [5,37].

THEOREM 3.1. Let $\mathcal{H}$ and $\mathcal{G}$ be Hilbert spaces, and $B : \mathcal{H}\times\mathcal{G}\to\mathbb{R}$ a bilinear functional with the following three properties:
(i) There exist a constant $M > 0$ such that

$$B(u,v)\leqslant M\|u\|_{\mathcal{H}}\|v\|_{\mathcal{G}}\,,\quad \forall\, u\in\mathcal{H},\ v\in\mathcal{G}\,,$$

where $\|.\|_{\mathcal{H}}$ and $\|.\|_{\mathcal{G}}$ denote the norms on $\mathcal{H}$ and $\mathcal{G}$, respectively.
(ii) There exist a constant $\gamma > 0$ such that

$$\inf_{\substack{u\in\mathcal{H}\\ \|u\|_{\mathcal{H}}=1}} \sup_{\substack{v\in\mathcal{G}\\ \|v\|_{\mathcal{G}}\leqslant 1}} |B(u,v)|\geqslant\gamma\,,$$

(iii) And

$$\sup_{u\in\mathcal{H}} |B(u,v)| > 0\,,\qquad v\neq 0\,,\quad v\in\mathcal{G}\,.$$

Let L be a continuous linear functional on $\mathcal{G}$. Then, there exist a unique solution to the following problem: Find $u\in\mathcal{H}$ such that

$$B(u,v) = L(v)\quad \forall\, v\in\mathcal{G}\,.$$

Moreover,

$$\|u\|_{\mathcal{H}}\leqslant\frac{1}{\gamma}\|L\|_{\mathcal{G}'}\,.$$

An approximation of (18) consists of constructing families of closed (generally finite dimensional) subspaces, $\mathcal{H}_h\subset\mathcal{H}$, $\mathcal{G}_h\subset\mathcal{G}$, and seeking solutions $u_h\in\mathcal{H}_h$ to the following problems:
Find $u_h\in\mathcal{H}_h$ such that

$$B(u_h,v_h) = L(v_h)\quad \forall\, v_h\in\mathcal{G}_h\,. \tag{19}$$

Let us assume that the conditions of Theorem 3.1 hold for problem (18), and that (19) is an approximation to (18). Then, $B(.,.)$ and $L(.)$ are continuous on $\mathcal{H}_h\times\mathcal{G}_h$ and $\mathcal{G}_h$, respectively. It follows that (19) is solvable if there exist $\gamma_h > 0$ such that

$$\inf_{\substack{u\in\mathcal{H}_h\\ \|u\|_{\mathcal{H}_h}=1}} \sup_{\substack{v\in\mathcal{G}_h\\ \|v\|_{\mathcal{G}_h}\leqslant 1}} |B(u,v)|\geqslant\gamma_h\,, \tag{20}$$

and

$$\sup_{u\in\mathcal{H}_h} |B(u,v)| > 0\,,\qquad v\neq 0\,,\quad v\in\mathcal{G}\,. \tag{21}$$

A straightforward calculation reveals that the error $u - u_h$ in the approximation (19) of (18) satisfies the estimate

$$\|u - u_h\|_{\mathscr{H}} \leq \left(1 + \frac{M}{\gamma_h}\right) \inf_{w \in \mathscr{H}_h} \|u - w\|_{\mathscr{H}}. \tag{22}$$

3.4. Natural norm

In this section we prove continuity of the bilinear form (16) with respect to the induced W-norm (11) which defines $W(\mathscr{P}_h)$ through the process of completion.

THEOREM 3.2. The bilinear form (16) can be bounded as follows:

$$B(u, v) \leq \|u\|_W \|v\|_W$$

where $\|.\|_W$ is the norm defined in (11).

PROOF. Let us first note that

$$\sum_{\Omega_e \in \mathscr{P}_h} \int_{\partial \Omega_e \backslash \Gamma_-} v(\boldsymbol{\beta} \cdot \boldsymbol{n}_e) u^- \, ds = \int_{\Gamma_{\text{int}}} [v](\boldsymbol{\beta} \cdot \boldsymbol{n}) u^- \, ds + \int_{\Gamma_+} v(\boldsymbol{\beta} \cdot \boldsymbol{n}) u \, ds,$$

then, we rewrite the bilinear form (16) as follows:

$$B(u, v) = \sum_{\Omega_e \in \mathscr{P}_h} \int_{\Omega_e} (\nabla v \cdot A\nabla u - (\nabla v \cdot \boldsymbol{\beta})u + v\sigma u) \, dx$$

$$+ \int_{\Gamma_+} v(\boldsymbol{\beta} \cdot \boldsymbol{n})u \, ds + \int_{\Gamma_D} ((A\nabla v) \cdot \boldsymbol{n} u - v(A\nabla u) \cdot \boldsymbol{n}) \, ds$$

$$+ \int_{\Gamma_{\text{int}}} (\langle (A\nabla v) \cdot \boldsymbol{n}\rangle [u] - \langle (A\nabla u) \cdot \boldsymbol{n}\rangle [v] + u^-(\boldsymbol{\beta} \cdot \boldsymbol{n})[v]) \, ds, \tag{23}$$

introducing scaling factors $(h^\alpha h^{-\alpha})$ where necessary and using Hölder's inequality, the above bilinear form can be bounded as follows:

$$B(u, v) \leq \|u\|_W \|v\|_W. \quad \square$$

3.5. Alternative definition of norms

Given that the natural norm $\|.\|_W$ is a mesh-dependent variant of the H^1 norm, to perform a study of convergence and stability of solutions in the L^2 norm we need to use different norms for the trial and test spaces. In this section we show how the bilinear form can be bounded utilizing one norm for the trial space, which is related to the L^2 norm, and another norm for the test space which is related to the H^2 seminorm. The set of norms to be presented in this section will be used to obtain an a priori error estimate of the error in the L^2 norm.

THEOREM 3.3. The bilinear form (16) can be bounded as follows:

$$B(u, v) \leq \|u\|_{W_1} \|v\|_{W_2}, \tag{24}$$

where

$$\|u\|_{W_j}^2 = \|u\|_{V_j}^2 + \|u\|_{\beta_j}^2 + \|u\sigma^{(j-1)}\|_{0,\Omega}^2, \quad j = 1, 2, \tag{25}$$

$$\|u\|_{V_1}^2 = |u|_{0,\mathscr{P}_h}^2 + |h^\alpha u|_{0,\Gamma_D \cup \Gamma_N}^2 + |h^\delta \alpha_1^{-1}(A\nabla u) \cdot \boldsymbol{n}|_{0,\Gamma_D}^2$$

$$+ |h^\alpha [u]|_{0,\Gamma_{\text{int}}}^2 + |h^\delta \alpha_1^{-1}\langle (A\nabla u) \cdot \boldsymbol{n}\rangle|_{0,\Gamma_{\text{int}}}^2 + |h^\alpha \langle u\rangle|_{0,\Gamma_{\text{int}}}^2, \tag{26}$$

$$\|v\|_{V_2}^2 = |v|_{2,\mathscr{P}_h}^2 + |h^{-\delta} \alpha_1 v|_{0,\Gamma_D}^2 + |h^{-\alpha} 2(A\nabla v) \cdot \boldsymbol{n}|_{0,\Gamma_D \cap \Gamma_N}^2 + |h^{-\delta} \alpha_1 [v]|_{0,\Gamma_{\text{int}}}^2$$

$$+ |h^{-\alpha} \langle 2(A\nabla v) \cdot \boldsymbol{n}\rangle|_{0,\Gamma_{\text{int}}}^2 + |h^{-\alpha} [(A\nabla v) \cdot \boldsymbol{n}]|_{0,\Gamma_{\text{int}}}^2, \tag{27}$$

$$|u|_{0,\mathscr{P}_h}^2 = \sum_{\Omega_e \in \mathscr{P}_h} \int_{\Omega_e} u^2 \, d\boldsymbol{x} \,, \quad |v|_{2,\mathscr{P}_h}^2 = \sum_{\Omega_e \in \mathscr{P}_h} \int_{\Omega_e} (\boldsymbol{\nabla} \cdot (A\boldsymbol{\nabla}v))^2 \, d\boldsymbol{x} \,,$$

$$|v|_{0,\Gamma}^2 = \int_\Gamma v^2 \, ds \,, \quad \text{for } \Gamma \in \{\Gamma_D, \Gamma_N, \Gamma_{\text{int}}\} \,,$$

and

$$\|u\|_{\beta_1}^2 = |h^\alpha u^+|_{0,\Gamma_-}^2 + |h^\alpha [u]|_{0,\Gamma_{\text{int}}}^2 + \|h u_\beta\|_{0,\Omega}^2 \,, \tag{28}$$

$$\|v\|_{\beta_2}^2 = |h^{-\alpha}|\beta_n|v^+|_{0,\Gamma_-}^2 + |h^{-\alpha}|\beta_n|v^+|_{0,\Gamma_{\text{int}}}^2 + \|h^{-1}|\beta|v\|_{0,\Omega}^2 \,, \tag{29}$$

with $\alpha = 1/2$, $\delta = 3/2$, $\beta_n = (\boldsymbol{\beta} \cdot \boldsymbol{n})$, $[u] = (u^- - u^+)$ *on* Γ_{int}, *and* $u_\beta = |\boldsymbol{\beta}|^{-1}(\boldsymbol{\nabla}u \cdot \boldsymbol{\beta})$ *when* $|\boldsymbol{\beta}| > 0$, *otherwise* $u_\beta = 0$. *In* $\|.\|_{V_j}$ *and* $\|.\|_{\beta_j}$ *the scaling parameter* h *is* $h_e/2$ *on* $\partial\Omega_e \cap \partial\Omega$, *and the average* $(h_e + h_f)/2$ *on* $\partial\Omega_e \cap \partial\Omega_f$.

PROOF. First, let us define a new set of norms for the diffusion operators. Considering only the diffusion terms in (16), we can use integration by parts on the first summation of the RHS to obtain

$$\sum_{\Omega_e \in \mathscr{P}_h} \int_{\Omega_e} \boldsymbol{\nabla}v \cdot A\boldsymbol{\nabla}u \, d\boldsymbol{x} = \int_{\Gamma_D} u(A\boldsymbol{\nabla}v) \cdot \boldsymbol{n} \, ds + \int_{\Gamma_N} u(A\boldsymbol{\nabla}v) \cdot \boldsymbol{n} \, ds$$

$$+ \int_{\Gamma_{\text{int}}} (\langle u\rangle[(A\boldsymbol{\nabla}v) \cdot \boldsymbol{n}] + \langle(A\boldsymbol{\nabla}v) \cdot \boldsymbol{n}\rangle[u]) \, ds - \sum_{\Omega_e \in \mathscr{P}_h} \int_{\Omega_e} u\boldsymbol{\nabla} \cdot (A\boldsymbol{\nabla}v) d\boldsymbol{x} \,,$$

and the diffusive part of the bilinear form can be rewritten as follows:

$$B(u, v) = -\sum_{\Omega_e \in \mathscr{P}_h} \int_{\Omega_e} u\boldsymbol{\nabla} \cdot (A\boldsymbol{\nabla}v) d\boldsymbol{x}$$

$$+ \int_{\Gamma_D} (2(A\boldsymbol{\nabla}v) \cdot \boldsymbol{n}u - v(A\boldsymbol{\nabla}u) \cdot \boldsymbol{n}) \, ds + \int_{\Gamma_N} (A\boldsymbol{\nabla}v) \cdot \boldsymbol{n}u \, ds$$

$$+ \int_{\Gamma_{\text{int}}} (2\langle(A\boldsymbol{\nabla}v) \cdot \boldsymbol{n}\rangle[u] - \langle(A\boldsymbol{\nabla}u) \cdot \boldsymbol{n}\rangle[v] + [(A\boldsymbol{\nabla}v) \cdot \boldsymbol{n}]\langle u\rangle) \, ds \,.$$

This bilinear form is now bounded using different norms for the test and trial functions. Looking for a norm on the trial space equivalent to the L^2-norm, we write

$$B(u, v) \leqslant |u|_{0,\mathscr{P}_h}^2 |v|_{2,\mathscr{P}_h}^2 + (|h^\alpha u|_{0,\Gamma_D \cup \Gamma_N}^2 + |h^\delta \alpha_1^{-1}(A\boldsymbol{\nabla}u) \cdot \boldsymbol{n}|_{0,\Gamma_D}^2 + |h^\alpha [u]|_{0,\Gamma_{\text{int}}}^2$$

$$+ |h^\delta \alpha_1^{-1}\langle(A\boldsymbol{\nabla}u) \cdot \boldsymbol{n}\rangle|_{0,\Gamma_{\text{int}}}^2 + |h^\alpha \langle u\rangle|_{0,\Gamma_{\text{int}}}^2)^{1/2}$$

$$\times (|h^{-\delta}\alpha_1 v|_{0,\Gamma_D}^2 + |h^{-\alpha}2(A\boldsymbol{\nabla}v) \cdot \boldsymbol{n}|_{0,\Gamma_D \cup \Gamma_N}^2 + |h^{-\delta}\alpha_1[v]|_{0,\Gamma_{\text{int}}}^2$$

$$+ |h^{-\alpha}\langle2(A\boldsymbol{\nabla}v) \cdot \boldsymbol{n}\rangle|_{0,\Gamma_{\text{int}}}^2 + |h^{-\alpha}[(A\boldsymbol{\nabla}v) \cdot \boldsymbol{n}]|_{0,\Gamma_{\text{int}}}^2)^{1/2}$$

and using the definitions of $\|.\|_{V_1}$ and $\|.\|_{V_2}$, we obtain

$$B(u, v) \leqslant \|u\|_{V_1}\|v\|_{V_2} \,. \tag{30}$$

Here again, we should note that the terms $h^{\pm\alpha}$ and $h^{\pm\delta}$ were introduced to minimize the mesh-dependence of an otherwise strongly mesh-dependent norm. For a uniform mesh, $\alpha = 1/2$ and $\delta = 3/2$ render a mesh-independent norm. From definition (26), we see that $\|.\|_{V_1}$ is closely related to the L^2-norm.

Let us now define a new set of norms for the convection terms. We first rewrite the bilinear form (convection terms only) as follows:

$$B(u, v) = \sum_{\Omega_e \in \mathscr{P}_h} \left\{ -\int_{\Omega_e} (\nabla v \cdot \boldsymbol{\beta}) u \, \mathrm{d}\boldsymbol{x} + \int_{\partial \Omega_e \backslash \Gamma_-} v(\boldsymbol{\beta} \cdot \boldsymbol{n}_e) u^- \, \mathrm{d}s \right\}$$

$$+ \sum_{\Omega_e \in \mathscr{P}_h} \left\{ -\int_{\partial \Omega_e} v(\boldsymbol{\beta} \cdot \boldsymbol{n}_e) u \, \mathrm{d}s + \int_{\Omega_e} v \nabla \cdot (\boldsymbol{\beta} u) \, \mathrm{d}\boldsymbol{x} + \int_{\partial \Omega_e \backslash \Gamma_-} v(\boldsymbol{\beta} \cdot \boldsymbol{n}_e) u^- \, \mathrm{d}s \right\}$$

$$= -\int_{\Gamma_-} v(\boldsymbol{\beta} \cdot \boldsymbol{n}) u \, \mathrm{d}s + \sum_{\Omega_e \in \mathscr{P}_h} \left\{ \int_{\Omega_e} v \nabla \cdot (\boldsymbol{\beta} u) \, \mathrm{d}\boldsymbol{x} + \int_{\partial \Omega_e \backslash \Gamma_-} v(\boldsymbol{\beta} \cdot \boldsymbol{n}_e)(u^- - u) \, \mathrm{d}s \right\}$$

$$= \int_{\Gamma_-} v |\boldsymbol{\beta} \cdot \boldsymbol{n}| u \, \mathrm{d}s + \int_{\Omega} v \nabla \cdot (\boldsymbol{\beta} u) \, \mathrm{d}\boldsymbol{x} - \int_{\Gamma_{\text{int}}} v^+ |\boldsymbol{\beta} \cdot \boldsymbol{n}| (u^- - u^+) \, \mathrm{d}s \; .$$

Introducing scaling factors $(h^\alpha h^{-\alpha})$ and $(h^\delta h^{-\delta})$ where appropriate and using Hölder's inequality, we obtain

$$B(u, v) \leqslant \sqrt{|h^\alpha u^+|^2_{0,\Gamma_-} + |h^\alpha [u]|^2_{0,\Gamma_{\text{int}}} + \|h u_\beta\|^2_{0,\Omega}}$$

$$\times \sqrt{|h^{-\alpha} |\beta_n| v^+|^2_{0,\Gamma_-} + |h^{-\alpha} |\beta_n| v^+|^2_{0,\Gamma_{\text{int}}} + \|h^{-1} |\beta| v\|^2_{0,\Omega}}$$

where $\beta_n = (\boldsymbol{\beta} \cdot \boldsymbol{n})$, $[u] = (u^- - u^+)$ on Γ_{int}, and $u_\beta = |\boldsymbol{\beta}|^{-1}(\nabla u \cdot \boldsymbol{\beta})$ when $|\boldsymbol{\beta}| > 0$, otherwise $u_\beta = 0$.
Using definitions (28) and (29), we obtain

$$B(u, v) \leqslant \|u\|_{\beta_1} \|v\|_{\beta_2} \; .$$

Finally, we have all the elements necessary to define a new set of norms for the convection–diffusion problem. Using the definitions of $\|.\|_{\beta_j}$, $j = 1, 2$, given in (28) and (29), and the definitions of $\|.\|_{V_j}$, $j = 1, 2$, given in (26) and (27), we can bound the bilinear form (23) as follows:

$$B(u, v) \leqslant \|u\|_{V_1} \|v\|_{V_2} + \|u\|_{\beta_1} \|v\|_{\beta_2} + \|u\|_{0,\Omega} \|v \sigma\|_{0,\Omega}$$

$$\leqslant \|u\|_{W_1} \|v\|_{W_2} \; .$$

By definition, $\|.\|_{W_1}$ is closely related to the L^2-norm, whereas $\|.\|_{W_2}$ resembles the H^2 − norm with two scaling parameters which are the local diffusivity and transport velocity $\square$.

3.6. Polynomial approximations on partitions

Let $\hat{\Omega}$ be a regular master element in $\mathbb{R}^d$; e.g. $\hat{\Omega} = (-1, 1)^d$. And let $\{F_{\Omega_e}\}$ be a family of invertible maps from $\hat{\Omega}$ onto Ω_e (see Fig. 2).
For every element $\Omega_e \in \mathscr{P}_h$, the finite-dimensional space of real-valued shape functions $\hat{P} \subset H^m(\hat{\Omega})$ is taken to be the space $P_{p_e}(\hat{\Omega})$ of polynomials of degree $\leqslant p_e$ defined on $\hat{\Omega}$. Then we define

$$P_{p_e}(\Omega_e) = \{\psi \mid \psi = \hat{\psi} \circ F_{\Omega_e}^{-1}, \hat{\psi} \in \hat{P} = P_{p_e}(\hat{\Omega})\} \; . \tag{31}$$

Using the spaces $P_{p_e}(\Omega_e)$, we can define the finite dimensional space

$$W_p(\mathscr{P}_h) = \prod_{e=1}^{N(\mathscr{P}_h)} P_{p_e}(\Omega_e), \qquad W_p(\mathscr{P}_h) \subset W(\mathscr{P}_h), \tag{32}$$

$N(\mathscr{P}_h)$ being the number of elements in partition $\mathscr{P}_h$.
The approximation properties of $W_p(\mathscr{P}_h)$ will be estimated using standard local approximation estimates (see [6]). Let $u \in H^s(\Omega_e)$; there exist a constant C depending on s and on the conditions (5) and (6), but independent of u, $h_e = \mathrm{diam}(\Omega_e)$, and p_e, and a polynomial u_p of degree p_e, such that for any $0 \leqslant r \leqslant s$ the following estimate hold:

$$\|u - u_p\|_{r,\Omega_e} \leqslant C \frac{h_e^{\mu-r}}{p_e^{s-r}} \|u\|_{s,\Omega_e}, \quad s \geqslant 0 , \tag{33}$$

where $\|.\|_{r,\Omega_e}$ denotes the usual Sobolev norm, and $\mu = \min(p_e + 1, s)$.
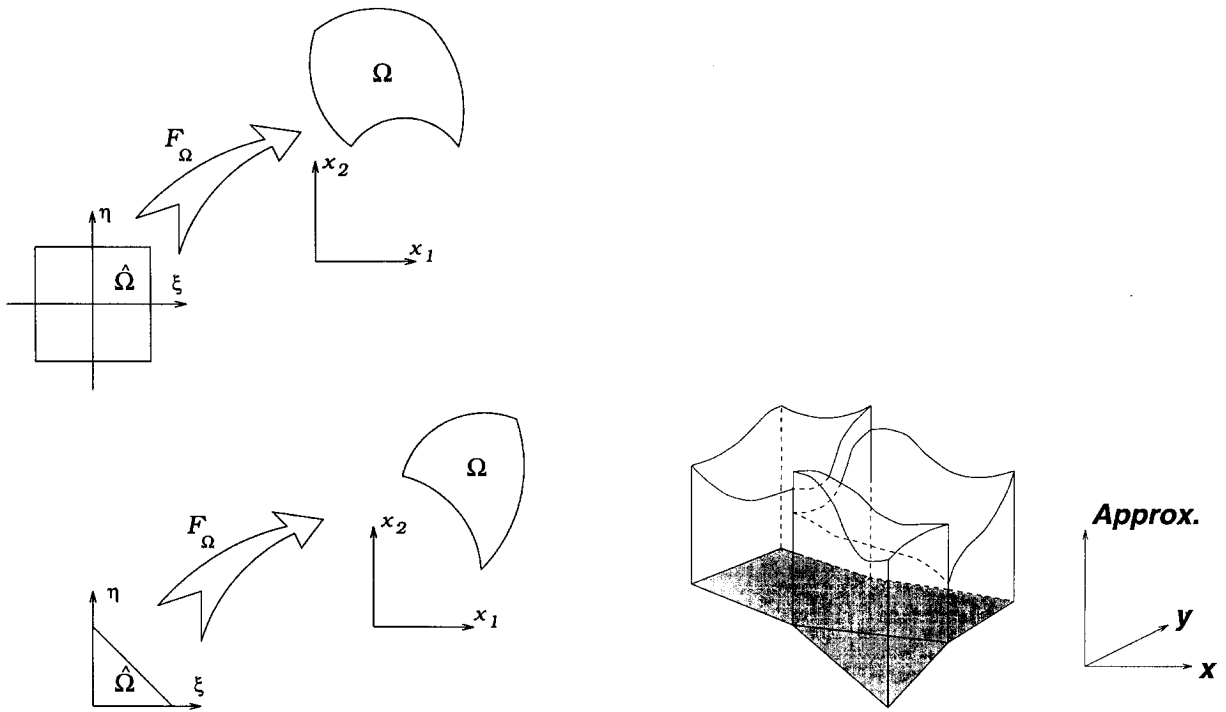
Fig. 2. Mappings $\Omega \to \Omega_e$ and discontinuous approximation.

3.7. Discontinuous Galerkin approximation

To construct approximations to the exact solution of problem (1)–(2) in a finite dimensional space, we use the following variational formulation in the space $W_p(\mathscr{P}_h)$:

$$
\boxed{
\begin{aligned}
&\text{Find } u_{\mathrm{DG}} \in W_p(\mathscr{P}_h) \text{ such that} \\
&B(u_{\mathrm{DG}}, v_h) = L(v_h) \quad \forall\, v_h \in W_p(\mathscr{P}_h)
\end{aligned}
}
\tag{34}
$$

where $B(.\,,.)$ and $L(.)$ are defined in (16) and (17), respectively.

The properties of the discontinuous Galerkin method presented in connection with (15) also hold for the finite dimensional approximation (34); namely, solutions are locally or elementwise conservative, the associated mass matrices are block diagonal, and the space of discontinuous functions provides the basis to obtain solutions with potentially better approximation properties in the L^2-norm.

Stability is one of the most important characteristics of a method for the solution of convection–diffusion problems. The following section addresses this issue and provides a priori error estimation for solutions of (34).

3.8. A priori error estimation

Convection–diffusion transport problems usually exhibit drastic changes in nature from diffusion dominated to convection dominated zones. The error of diffusion dominated problems is better measured in the H^1 norm because the associated physics depends on the solution gradient, such as heat transfer, viscous stresses, etc.; whereas the error in convection dominated transport is better measured in the L^2-norm, because the underlying physics depends almost exclusively on the solution values rather than on its gradient.

The range of local Pe values [0, 1) represents a class of problems in which diffusion is dominant, and for which the W-norm converges to the V-norm as Pe $\to 0$. The analysis of stability in the V-norm for diffusion

dominated problems was presented in [10,38], where optimal *h*-convergence rates are presented. For completeness, Section 4 includes a numerical example which shows optimal convergence rate in the *W*-norm.

The following theorem presents an a priori error estimate for the range of high Pe number, where convection is important. The reaction coefficient σ is assumed to be zero, this is the worst case scenario because when $\sigma > 0$ the problem is more stable.

THEOREM 3.4. *Let the solution to (15) be* $u \in H^s(\mathcal{P}_h(\Omega))$, *with* $s > 3/2$, *and assume that there exists* $\kappa \geq 0$ *and* $C_p > 0$ *such that*

$$\inf_{\substack{u \in W_1 \\ \|u\|_{W_1} \leq 1}} \sup_{\substack{v \in W_1 \\ \|v\|_{W_1} \leq 1}} |B(u, v)| \geq C_p p_{\max}^{-\kappa}, \tag{35}$$

where $p_{\max} = \max_e(p_e)$. *If the approximation estimate (33) holds for the spaces* $W_p(\mathcal{P}_h)$, *then the error of the approximate solution* u_{DG} *can be bounded as follows:*

$$\|u - u_{\mathrm{DG}}\|_{W_1}^2 \leq C p_{\max}^{2\kappa} \sum_{\Omega_e \in \mathcal{P}_h} \left(\frac{h_e^{\mu_e - \epsilon}}{p_e^{s - 3/2 - \epsilon}} \|u\|_{s, \Omega_e} \right)^2, \tag{36}$$

where $\mu_e = \min(p_e + 1, s)$, $\epsilon > 0$ *arbitrarily small,* $p_e \geq 1$, *and the constant C depends on s and on conditions (5) and (6), but it is independent of* u, h_e *and* p_e.

PROOF. Let us first bound $\|u\|_{V_1}$ and $\|u\|_{\beta_1}$ as follows:

$$\|u\|_{V_1}^2 \leq C_1 \sum_{\Omega_e \in \mathcal{P}_h} (\|u\|_{0, \Omega_e}^2 + h\|u\|_{1/2 + \epsilon, \Omega_e}^2 + h^3 \|u\|_{3/2 + \epsilon, \Omega_e}^2) \tag{37}$$

$$\|u\|_{\beta_1}^2 \leq C_2 \sum_{\Omega_e \in \mathcal{P}_h} (h\|u\|_{1/2 + \epsilon, \Omega_e}^2 + h^2 |u|_{1, \Omega_e}^2), \tag{38}$$

and using (37)–(38), we bound $\|u\|_{W_1}$:

$$\|u\|_{W_1}^2 \leq C \sum_{\Omega_e \in \mathcal{P}_h} (\|u\|_{0, \Omega_e}^2 + h^2 |u|_{1, \Omega_e}^2 + h\|u\|_{1/2 + \epsilon, \Omega_e}^2 + h^3 \|u\|_{3/2 + \epsilon, \Omega_e}^2). \tag{39}$$

Let $u_p \in W_p(\mathcal{P}_h)$ be a polynomial that approximates $u \in H^s(\mathcal{P}_h(\Omega))$ in the norm $\|.\|_{W_1}$. To obtain an upper bound of $\|u - u_p\|_{W_1}$, we use (39) and bound each of the four terms in the summation using (33) so that the exponent of *h* is the same in each term. Thus, we obtain:

$$\|u - u_p\|_{W_1}^2 \leq C \sum_{\Omega_e \in \mathcal{P}_h} \left(\frac{h_e^{\mu_e - \epsilon}}{p_e^{s - 3/2 - \epsilon}} \|u\|_{s, \Omega_e} \right)^2, \quad s > 3/2, \qquad \mu_e - \min(p_e + 1, s), \quad \epsilon > 0.$$

Finally, using the continuity and inf–sup parameters in (22), we arrive at the following a priori error estimate:

$$\|u - u_{\mathrm{DG}}\|_{W_1}^2 \leq \left(1 + \frac{M}{\gamma_h}\right)^2 \inf_{w_p \in W_p} \|u - w_p\|_{W_1}^2 \leq C p_{\max}^{2\kappa} \sum_{\Omega_e \in \mathcal{P}_h} \left(\frac{h_e^{\mu_e - \epsilon}}{p_e^{s - 3/2 - \epsilon}} \|u\|_{s, \Omega_e} \right)^2,$$

where $s > 3/2$, $\epsilon > 0$ arbitrarily small, $\mu_e = \min(p_e + 1, s)$, and *C* depends on *s* but is independent of u, h_e, and p_e. $\square$

The error estimate (36) is a bound for the worst possible case, including all possible data. For a wide range of data, however, the error estimate (36) may be pessimistic, and the actual rate of convergence can be larger than that suggested by the above bound.
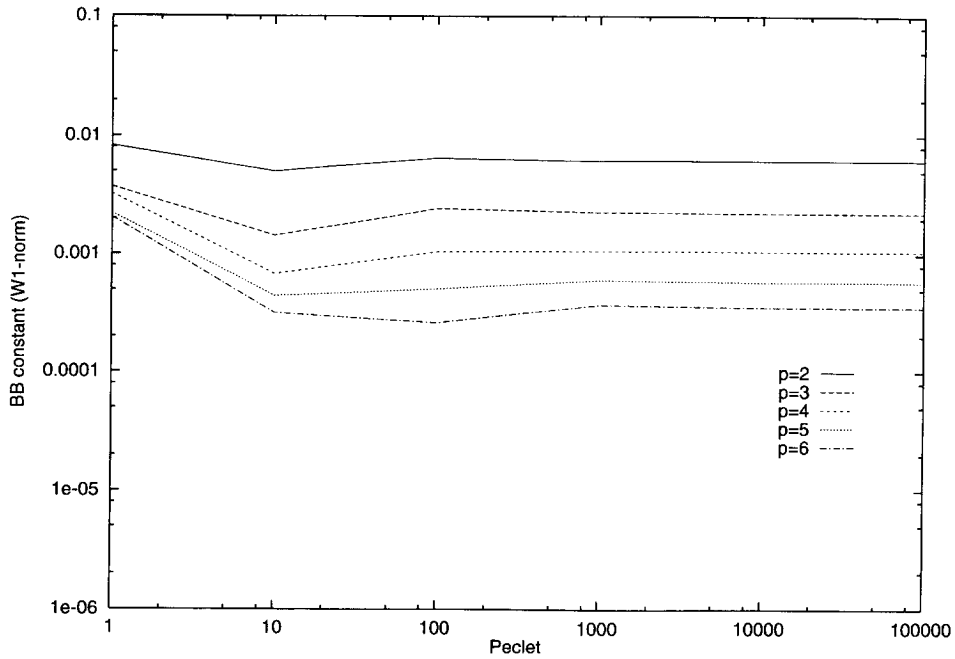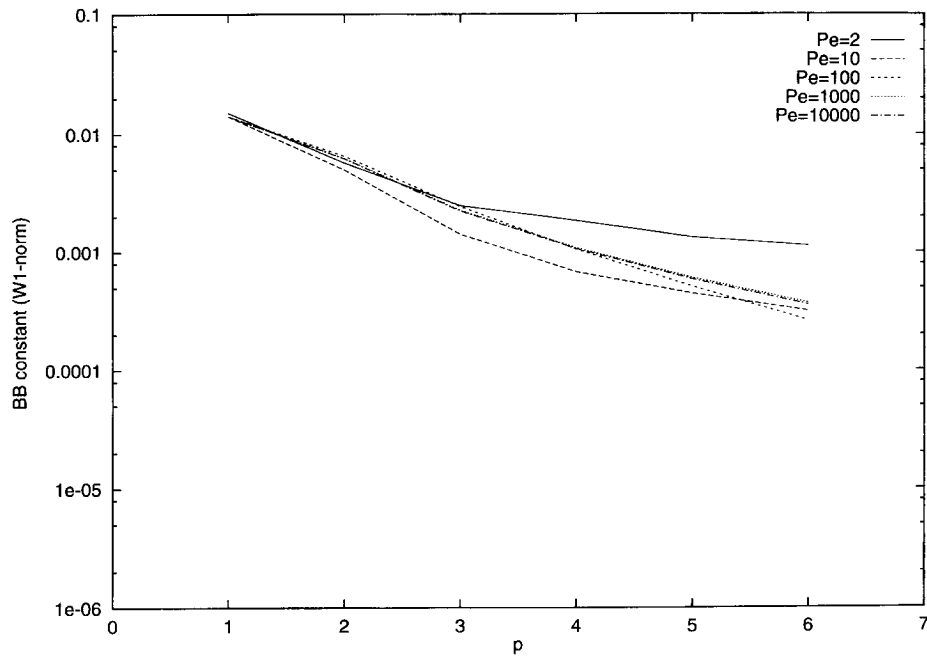
Fig. 3. BB(W_1) vs. Peclet, discontinuous Galerkin.

3.9. Numerical evaluation of the inf–sup condition

The numerical evaluation of the Inf–Sup parameter γ_h associated with the norm $\|.\|_{W_1}$ was done as described in [10,38]. The bilinear form (16) with $\sigma = 0$ was discretized in a one-dimensional setting with Dirichlet boundary conditions using different number of elements $N(\mathcal{P}_h)$ and uniform $p_e = p$, $1 \leqslant e \leqslant N(\mathcal{P}_h)$.

Figs. 3 and 4 show the Inf–Sup parameter γ_h as a function of the Peclet number $\mathrm{Pe} = |\beta| h / \alpha$ for different
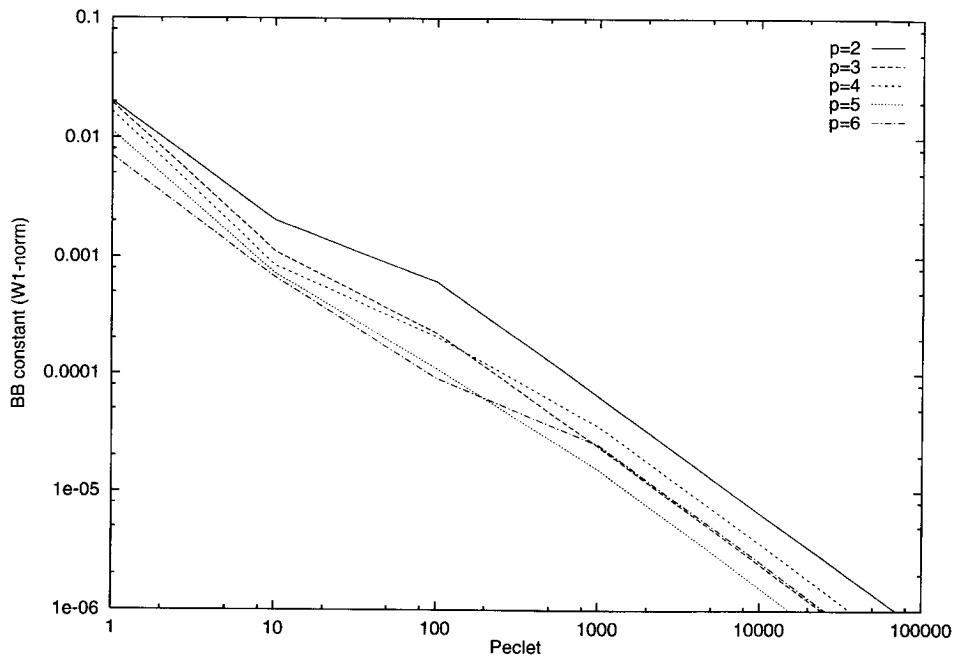
Fig. 4. BB(W_1) vs. Peclet, continuous Galerkin.

Fig. 5. BB(W_1) vs. spectral order, discontinuous Galerkin.

polynomial orders p, Fig. 3 corresponds to the DG method and Fig. 4 to the continuous C^0 Galerkin method. Figs. 5 and 6 shows the Inf–Sup parameter γ_h as a function of p for several values of Pe number. These figures show that the C^0 Galerkin method is unstable for large Pe numbers (a well-known fact) because the Inf–Sup parameter γ_h is inversely proportional to the Pe number. The DG method, however, is stable; the Inf–Sup parameter γ_h decreases only up to a given value when Pe increases.
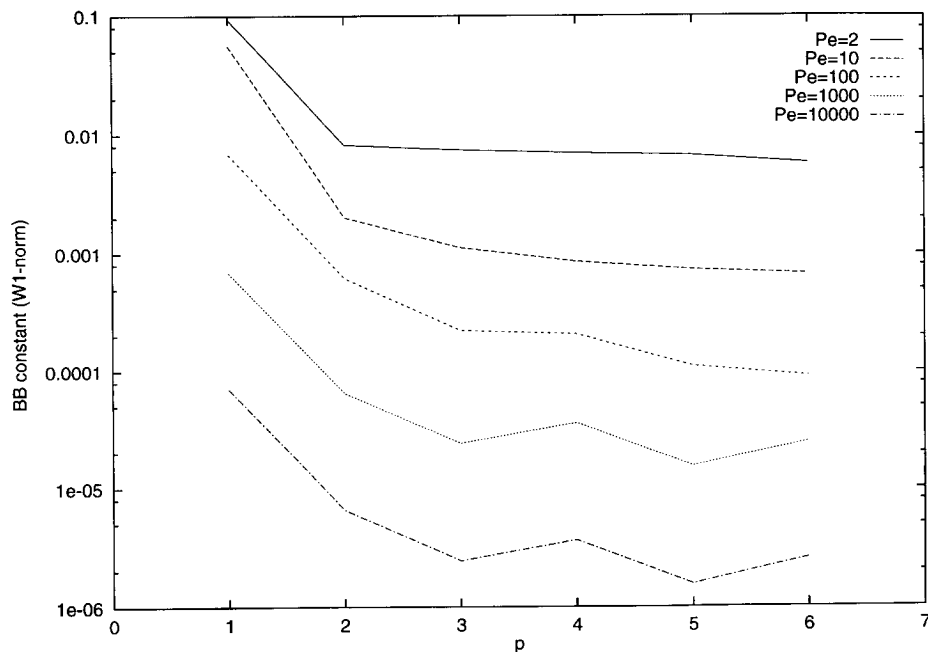
Fig. 6. BB(W_1) vs. spectral order, continuous Galerkin.

4. Numerical tests

4.1. Scalar convection–diffusion problems

First, the h-convergence rate is evaluated solving the following convection–diffusion problem

$$\begin{cases} -\alpha \dfrac{\partial^2 u}{\partial x^2} + \dfrac{\partial u}{\partial x} = \alpha(4\pi)^2 \sin(4\pi x) + 4\pi \cos(4\pi x) & \text{on } [0, 1] \\ u(x) = 0 & \text{at } x = 0 \text{ and } x = 1 \end{cases} \tag{40}$$

for which the exact solution is $u_{\text{exact}}(x) = \sin(4\pi x)$.

The h-convergence rate (accuracy) is given by

$$CR_h = \frac{\log(e_{2h}/e_h)}{\log(2)}, \qquad e_h = \|u_h - u_{\text{ex}}\|_{W_j}.$$

The analysis of error in the solution of problem (40) with $\alpha = 10^2$ is presented in Fig. 7, which shows the W-norm of the error, and Fig. 8 shows the h-convergence rate for uniform meshes. The asymptotic convergence rate in this H^1 like norm is of order $O(h^p)$, which is optimal from the approximation point of view.

Fig. 9 shows the error in the solution of (40) with $\alpha = 10^{-2}$. In this case the error is measured in the W_1-norm, which is an L^2-like norm, and Fig. 10 shows an h convergence rate of order $O(h^{p+1})$, which is again an optimal convergence rate from the approximation standpoint. This order of convergence rate is in agreement with the error estimate (36).

The next test cases involve the solution to the following singularly perturbed convection–diffusion problem

$$\begin{cases} -\alpha \dfrac{\partial^2 u}{\partial x^2} + \dfrac{\partial u}{\partial x} = S & \text{on } [0, 1] \\ u(0) = 1 \qquad u(1) = 0 \end{cases} \tag{41}$$

where $S = \{0, 1\}$, and the corresponding exact solutions are $u_{\text{exact}}(x) = \{1, x\} - (\exp(x/\alpha) - 1)/(\exp(1/\alpha) - 1)$.

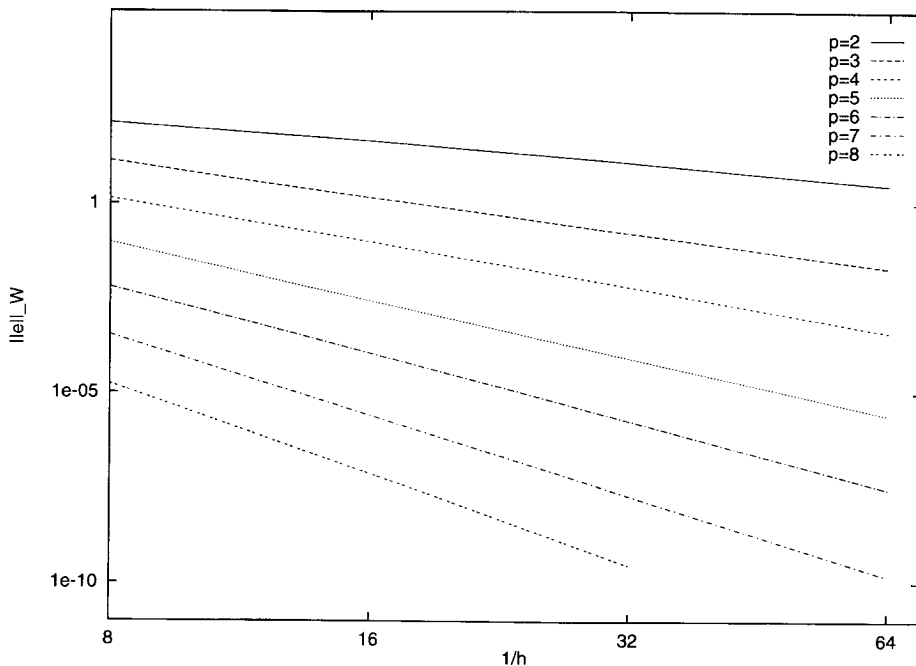The domain is discretized with 10 elements ($h = 1/10$), and $\alpha = h/\text{Pe}$. Fig. 11 shows the DG solution for

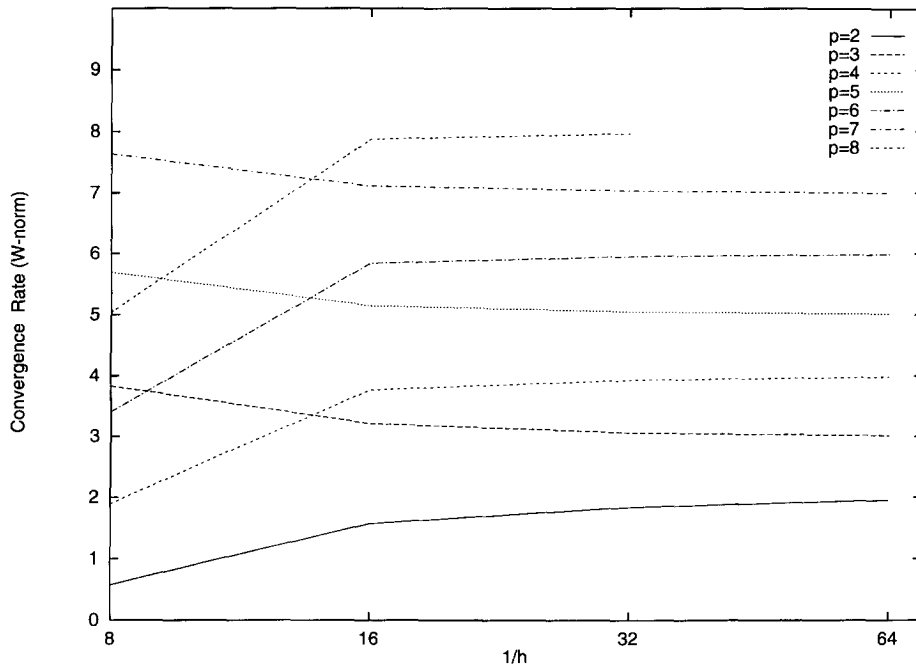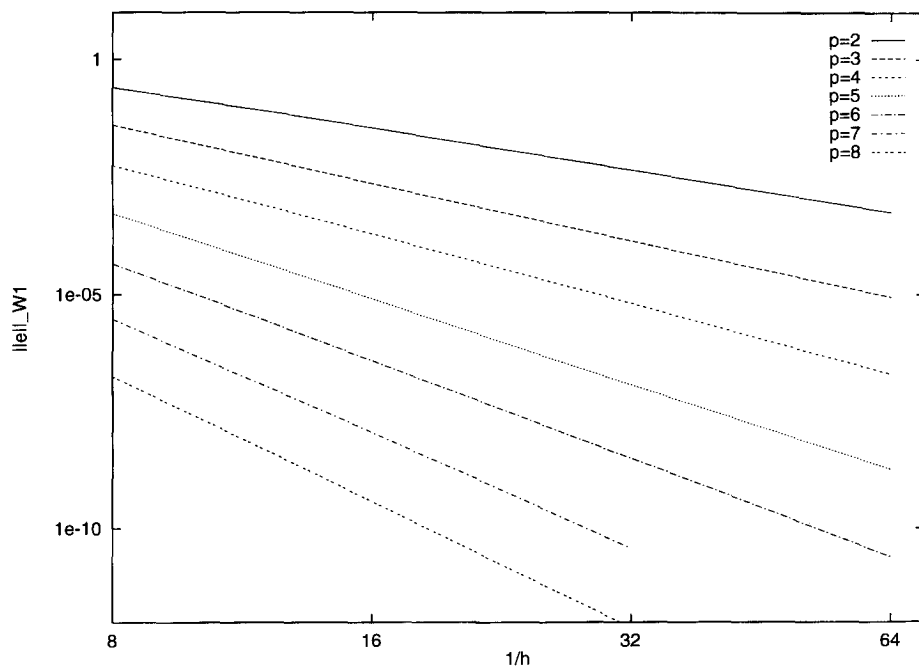Fig. 7. W-norm of the error: $-10^2 \, \partial^2 u/\partial x^2 + \partial u/\partial x = S$.

Fig. 8. H convergence rate: $-10^2 \, \partial^2 u/\partial x^2 + \partial u/\partial x = S$.

$S = 0$ and $\mathrm{Pe} = 10$, and Fig. 12 is a close up view of the two rightmost elements. These figures show cualitatively the weak approximation of Dirichlet boundary conditions. This type of approximation is fundamentally different from approximations in the H^1 norm; as it is shown in the following examples, in the presence of under-resolved boundary layers the DG approximation does not pollute the entire domain with spurious oscillations, and the approximation in the L^2-norm is very good.

Fig. 9. W_1-norm of the error: $-10^2 \, \partial^2 u/\partial x^2 + \partial u/\partial x = S$.
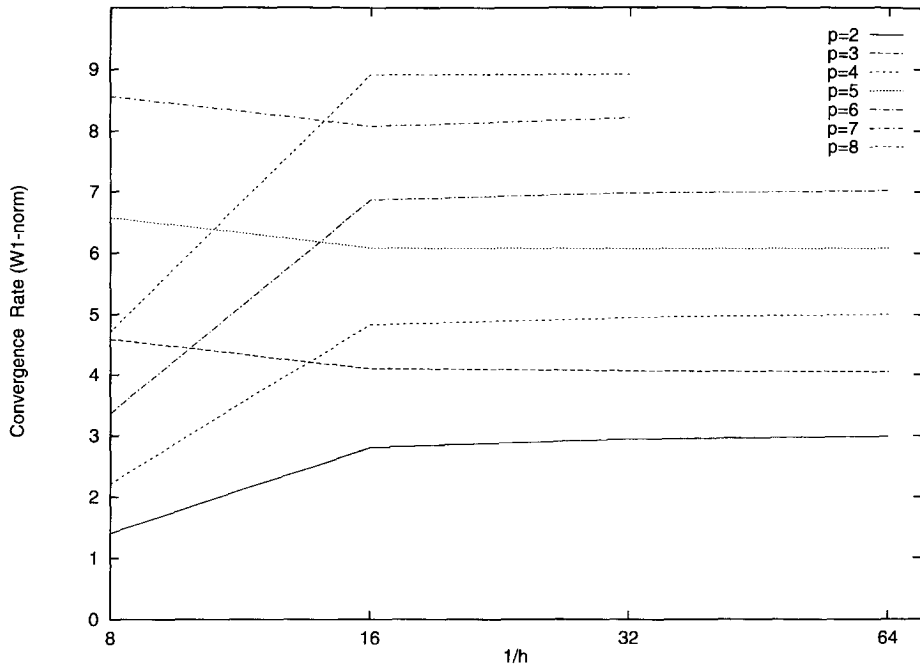
Fig. 10. H convergence rate: $-10^2\,\partial^2 u/\partial x^2 + \partial u/\partial x = S$.

Fig. 13 shows the solution for $S = 1$ and $Pe = 100$ obtained with the DG method, and Fig. 14 shows the same solution at the rightmost elements. Fig. 15 shows the solution to the same problem obtained with the *continuous* Galerkin method, and Fig. 16 shows this solution at the rightmost elements. Note that the oscillations of the continuous Galerkin method pollute the entire domain, whereas the DG method only presents small oscillation on the rightmost element, almost without pollution in the rest of the domain. This is very important for adaptive
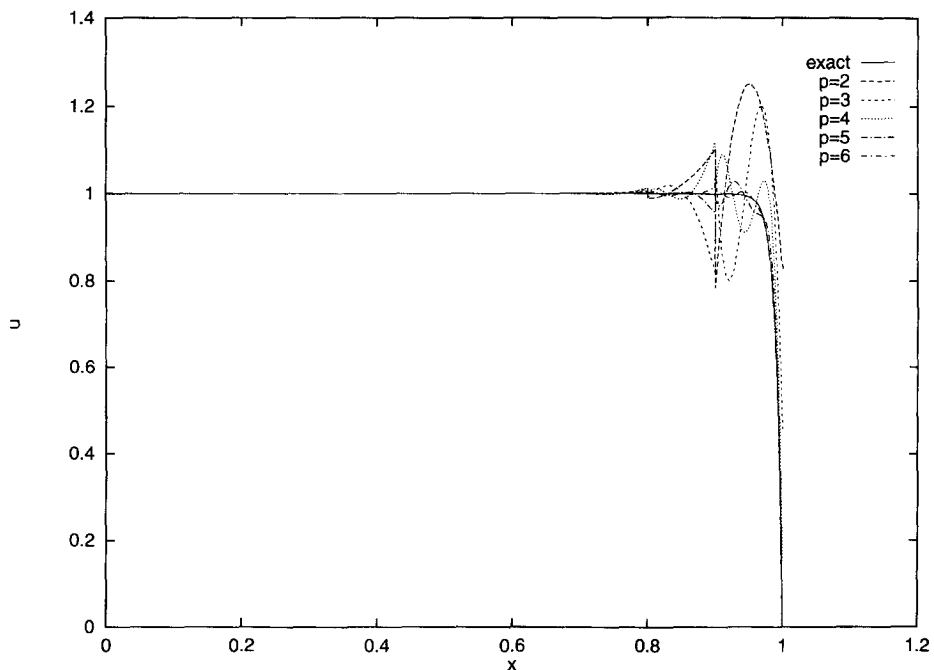
Fig. 11. Discontinuous Galerkin: $h = 1/10$, $Pe = 100$.
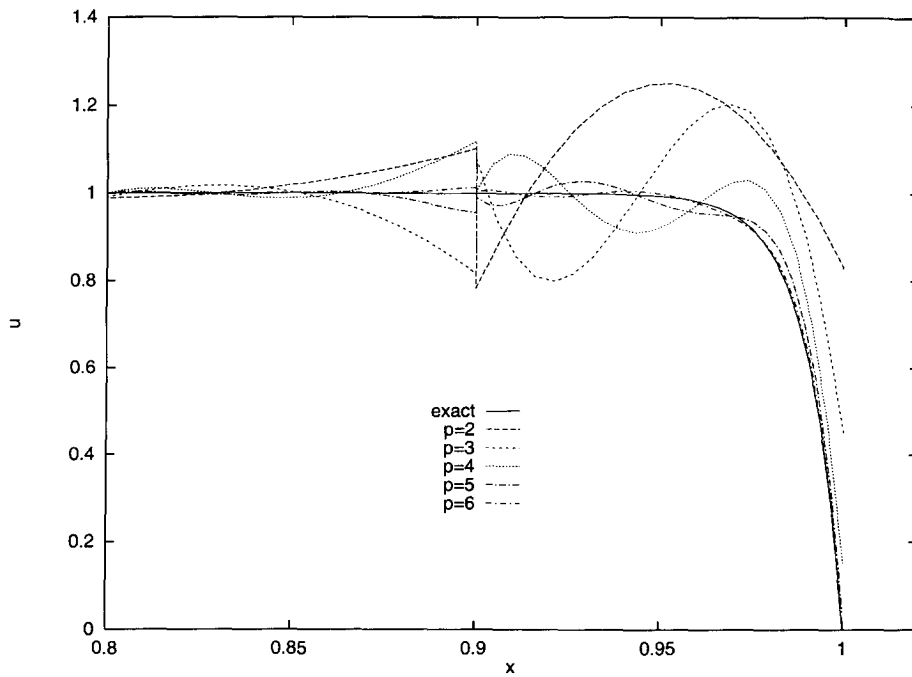
Fig. 12. Discontinuous Galerkin (rightmost elements): $h = 1/10$, Pe = 100.

strategies, because error indicators for the DG technique are very simple and accurate due to the lack of pollution in the solution.

Now, we present the solution to a convection–diffusion problem with a turning point in the middle of the domain. The Hemker problem is given as follows:
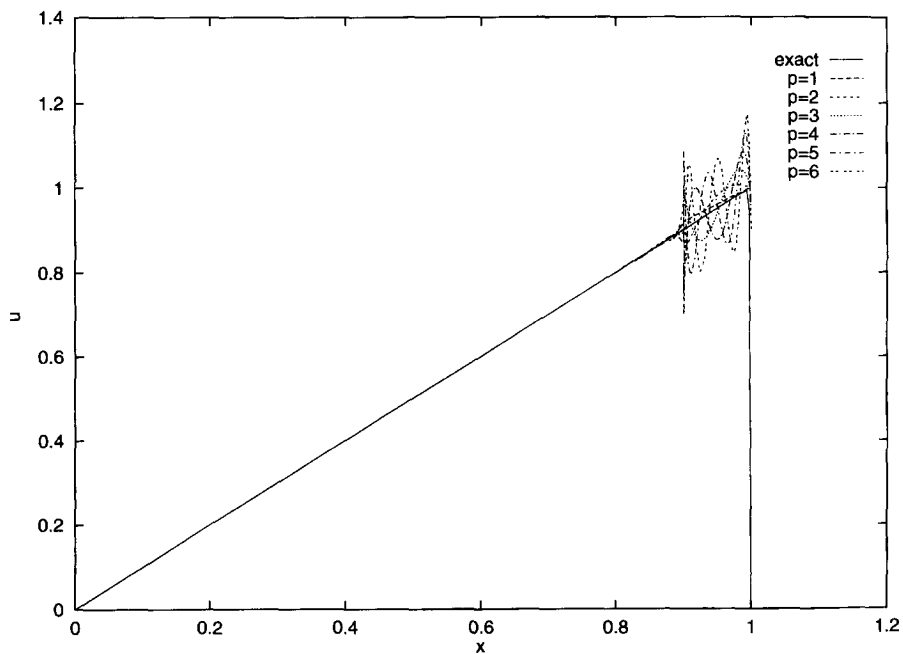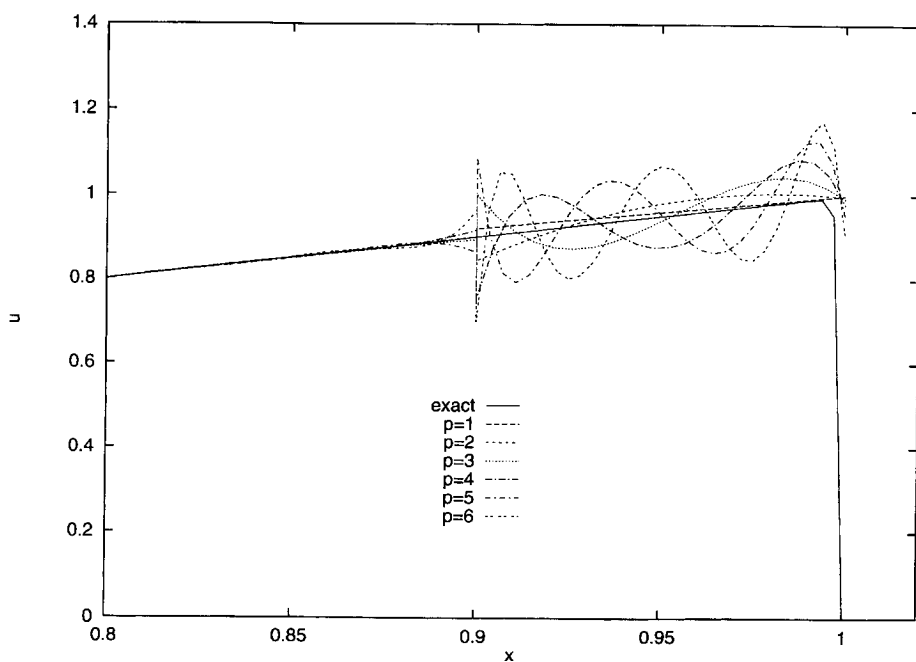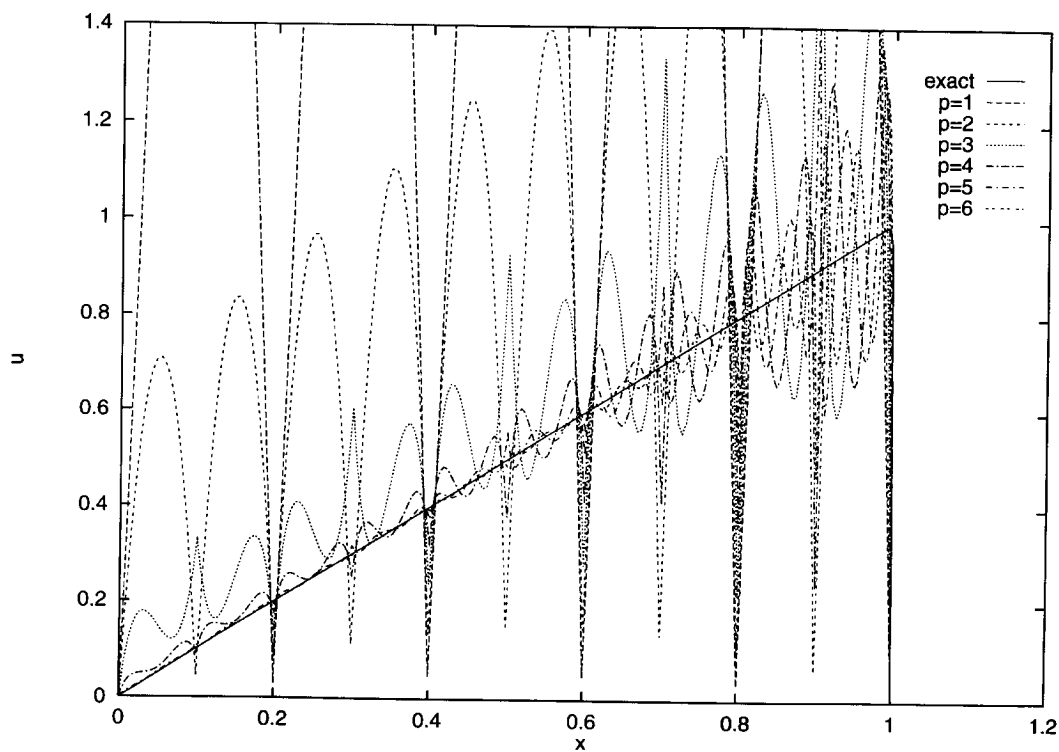

Fig. 13. Discontinuous Galerkin: $h = 1/10$, Pe = 100.

Fig. 14. Discontinuous Galerkin (rightmost elements): $h = 1/10$, Pe $= 100$.

$$\begin{cases} \alpha \dfrac{\partial^2 u}{\partial x^2} + x \dfrac{\partial u}{\partial x} = -\alpha \pi^2 \cos(\pi x) - \pi x \sin(\pi x) \quad \text{on } [0, 1] \\ u(-1) = -2, \qquad u(1) = 0 \end{cases} \tag{42}$$

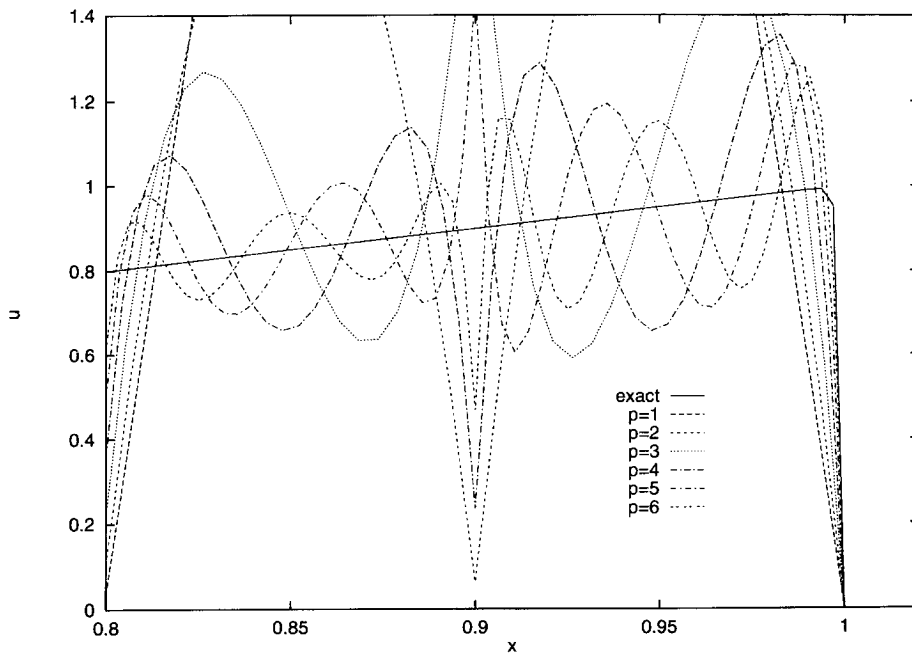Fig. 15. Continuous Galerkin: $h = 1/10$, Pe $= 100$.

Fig. 16. Discontinuous Galerkin (rightmost elements): $h = 1/10$, Pe = 100.

for which the exact solution is

$$u(x) = \cos(\pi x) + \mathrm{erf}(x/\sqrt{2\alpha})/\mathrm{erf}(1/\sqrt{2\alpha}).$$

Figs. 17 and 18 show solutions to the above problem ($\alpha = 10^{-10}$ and $h = 1/10$) obtained with continuous and discontinuous Galerkin, respectively.
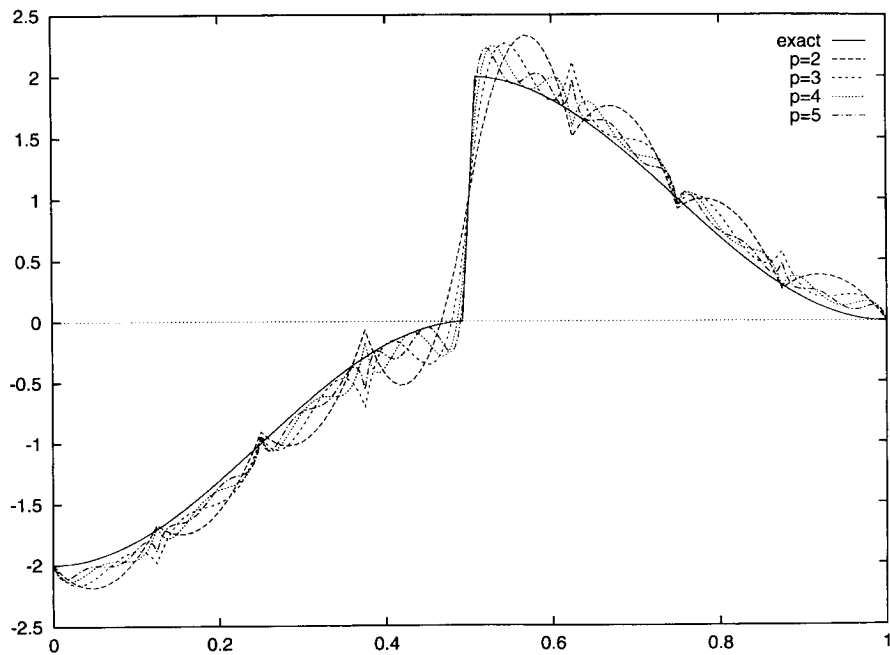

Fig. 17. Hemker problem: $\alpha = 10^{-10}$ and $h = 1/10$, continuous Galerkin.

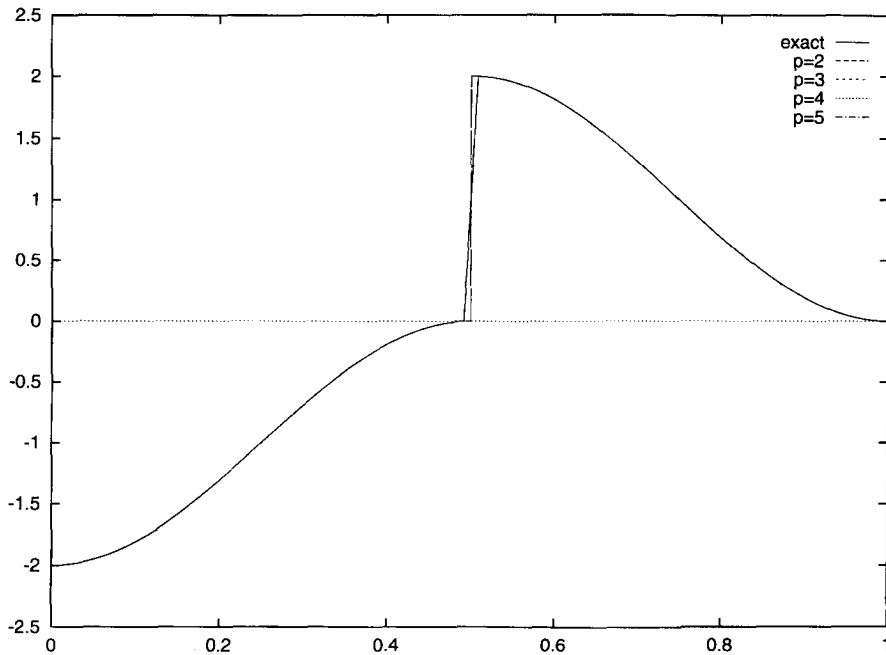Fig. 18. Hemker problem: $\alpha = 10^{-10}$ and $h = 1/10$, discontinuous Galerkin.

The numerical experiments show that for cases where the best approximation to the exact solution in the L^2-norm is better represented using discontinuous functions, the DG method performs better than the continuous Galerkin method. This is in general true for solutions to convection dominated problems with boundary layers. If the quantity of interest is the gradient of the solution at the boundary layers, the DG method provides an excellent error indicator which allows to capture steep gradients using adaptive refinement.

The next test case involves a two-dimensional irrotational incompressible flow around a cylinder with center at $(0,0)$, radius 1, and undisturbed flow velocity $(1,0)$. For this case, the exact solution given in terms of the stream function is

$$\psi = y \left(1 - \frac{1}{x^2 + y^2} \right),$$

and the velocity field is given by $u = \partial \psi / \partial y$, and $v = -\partial \psi / \partial x$. The value of the stream function ψ does not change along a streamline
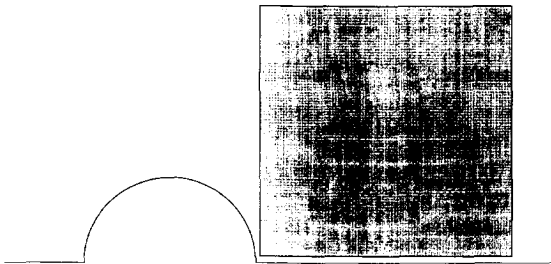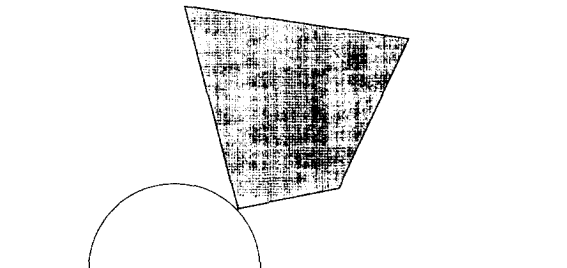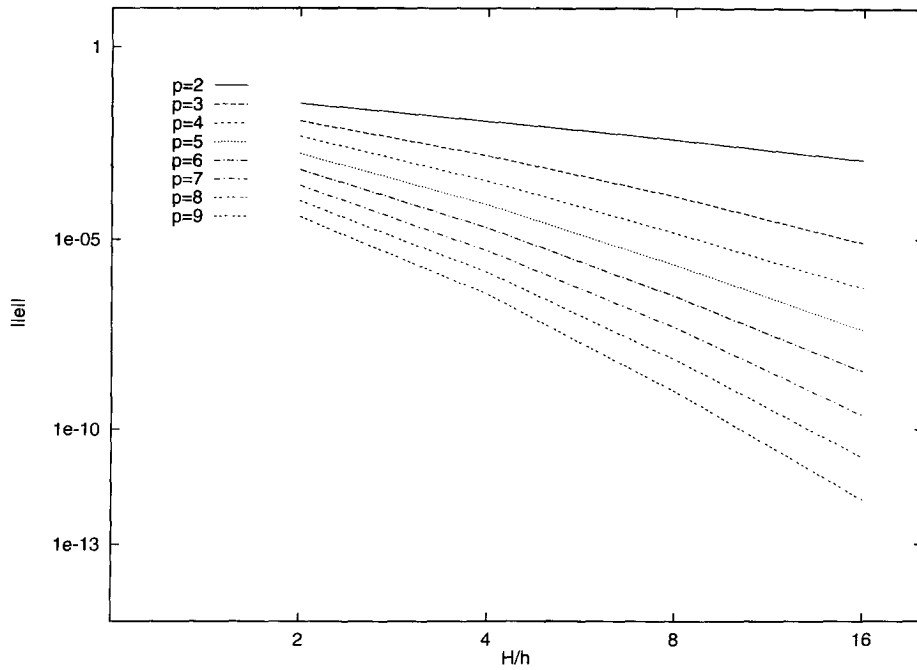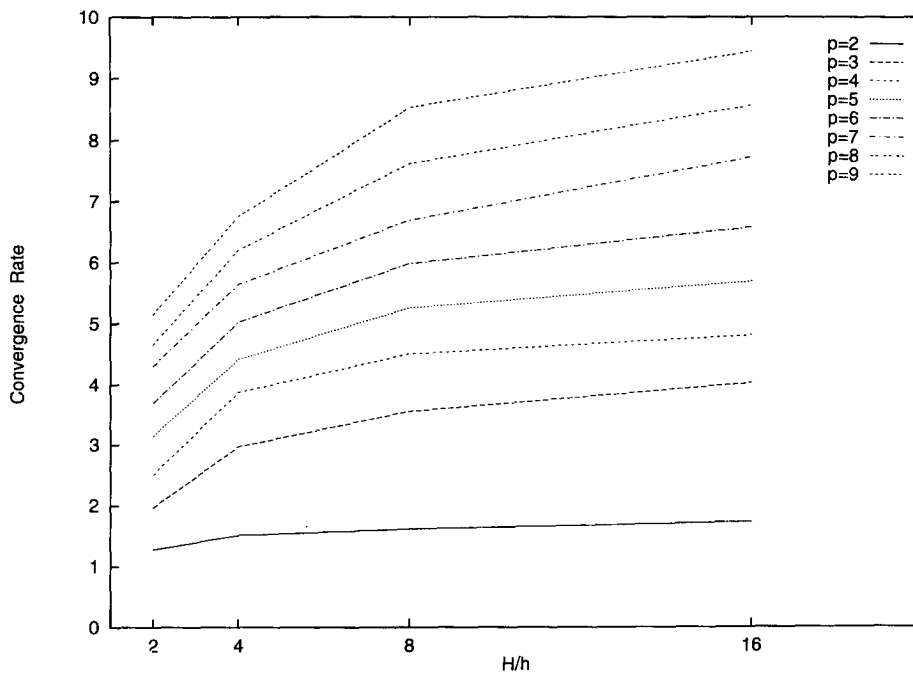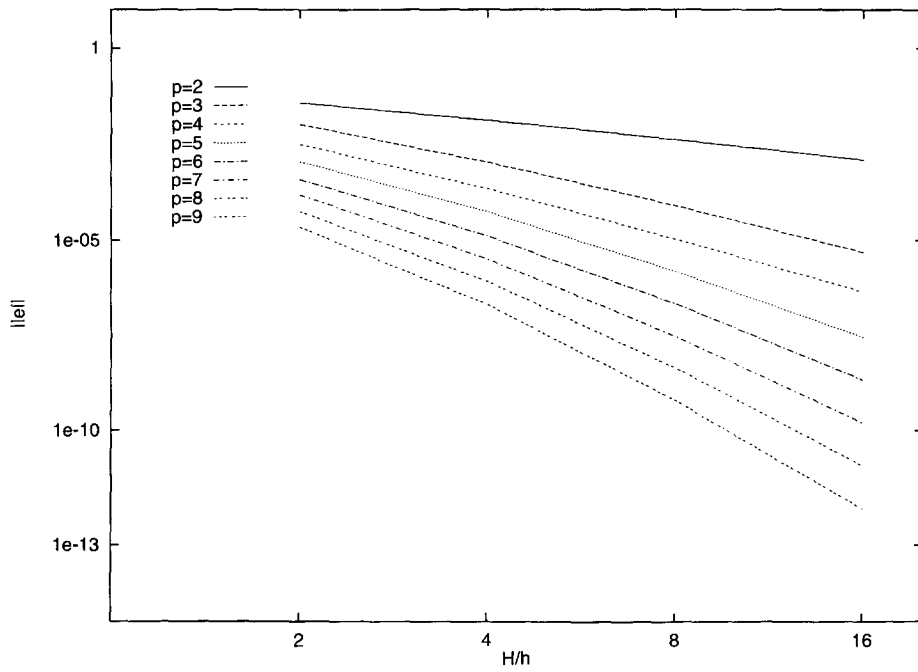

Fig. 19. Subdomain A.

Fig. 20. Subdomain B.
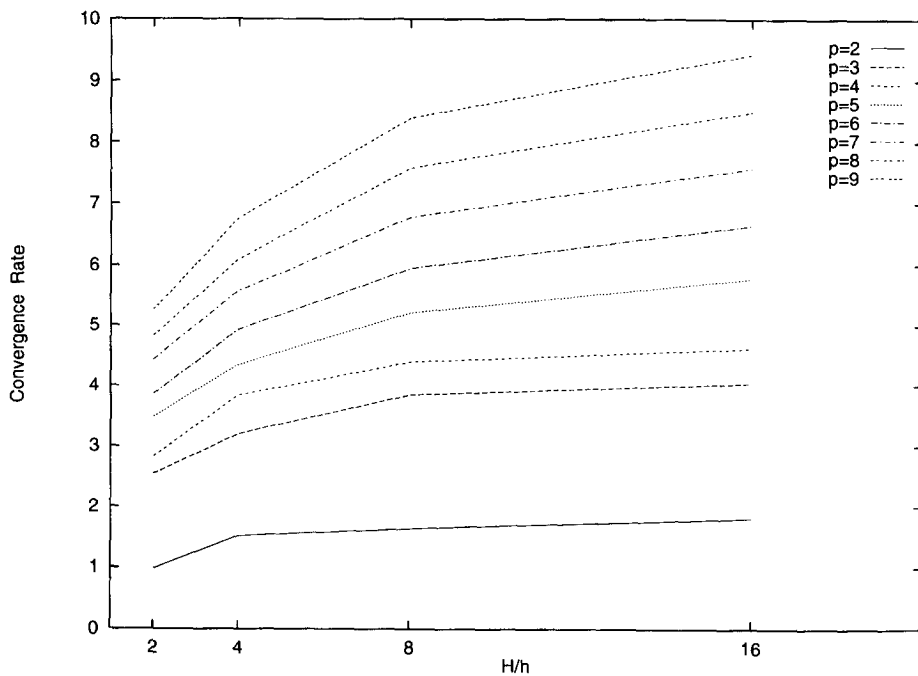
Fig. 21. L^2-norm of the error on subdomain A.

$$u\,\frac{\partial \psi}{\partial x} + v\,\frac{\partial \psi}{\partial y} = 0\,,$$

and ψ is also a solenoidal field, namely, it satisfies the condition $\Delta\psi = 0$. Therefore, we can set the following convection diffusion problem: Find ψ such that

Fig. 22. Convergence rate in L^2-norm on subdomain A.

Fig. 23. L^2-norm of the error on subdomain B.

$$\begin{cases} -\Delta \psi + u\, \dfrac{\partial \psi}{\partial x} + v\, \dfrac{\partial \psi}{\partial y} = 0, & \text{in } \Omega \\[2mm] \psi = y\left(1 - \dfrac{1}{x^2 + y^2} \right) & \text{on } \partial \Omega, \end{cases} \tag{43}$$

Fig. 24. Convergence rate in L^2-norm on subdomain B.
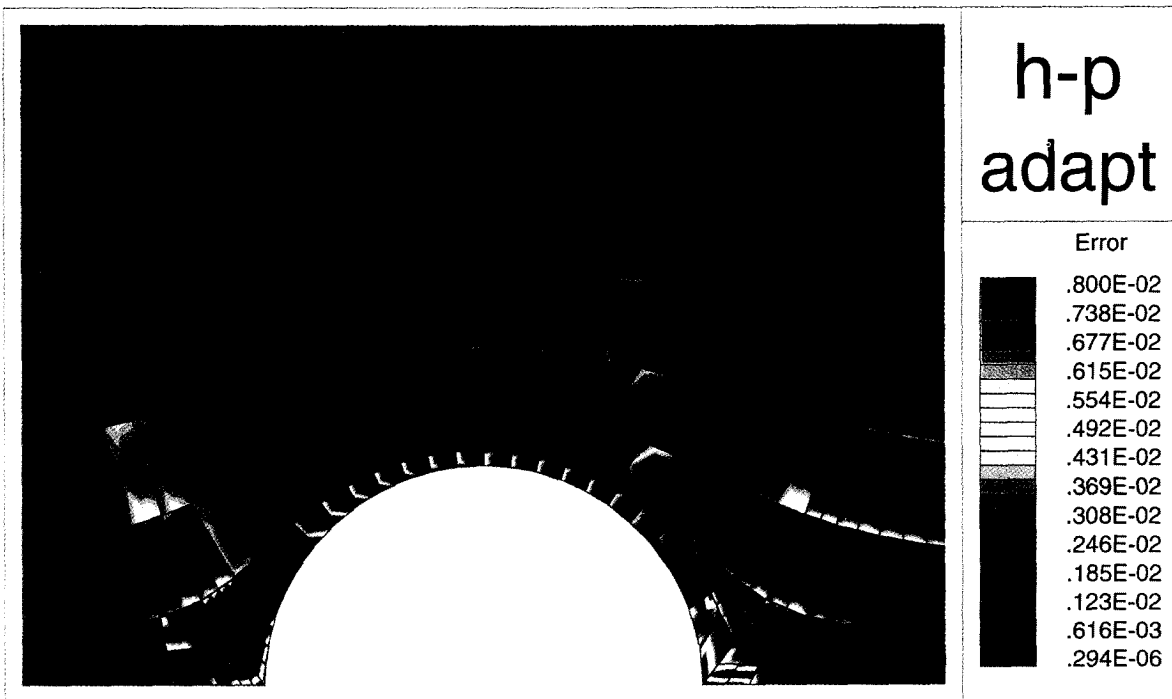
Fig. 25. Pointwise error with adaptive refinement: max $p_e = 1$.
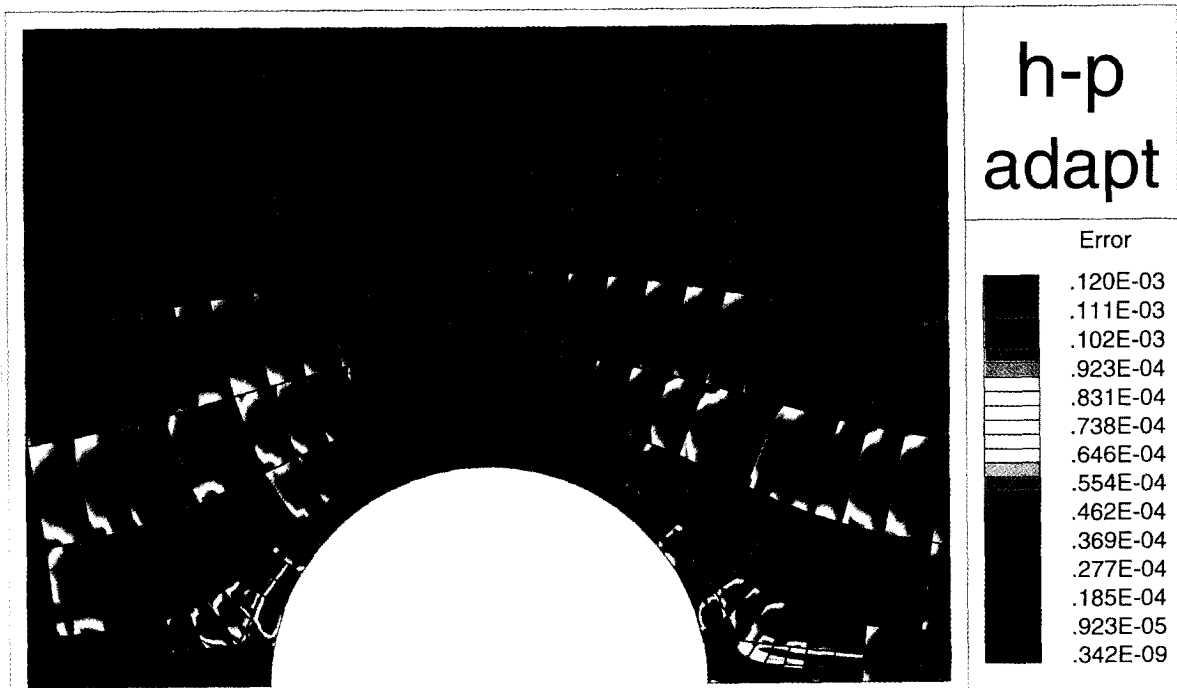
Fig. 26. Pointwise error with adaptive refinement: max $p_e = 3$.

where

$$u = 1 - \frac{(x^2 - y^2)}{(x^2 + y^2)^2}, \quad \text{and} \quad v = \frac{-2xy}{(x^2 + y^2)^2}$$

are given in Ω. The numerical evaluation of h-convergence rates (accuracy) is done on the subdomains shown in Figs. 19 and 20.

Fig. 21 shows the L^2-norm of the error and Fig. 22 h convergence rate for uniform refinements of subdomains A. Figs. 23 and 24 are the counterparts on subdomain B. For low p the convergence rate is $O(h^{p+1})$ for p odd and $O(h^p)$ for p even. For high p, however, the tendency seems to be towards a convergence rate of order $O(h^{p+1})$ regardless of p, but the asymptotic convergence rate is not reached for high p in the finest mesh due to round-off errors.

Figs. 25 and 26 show pointwise error in the solution of problem (43) using adaptive refinement with a max order $p_e = 1$ and $p_e = 3$, respectively. From these figures it is noticeable the reduction in pointwise error with the increase in polynomial order.

Summarizing, the numerical experiments confirm the stability and high accuracy that the method can deliver for the class of problems considered, including the use of h refinements and p enrichments.
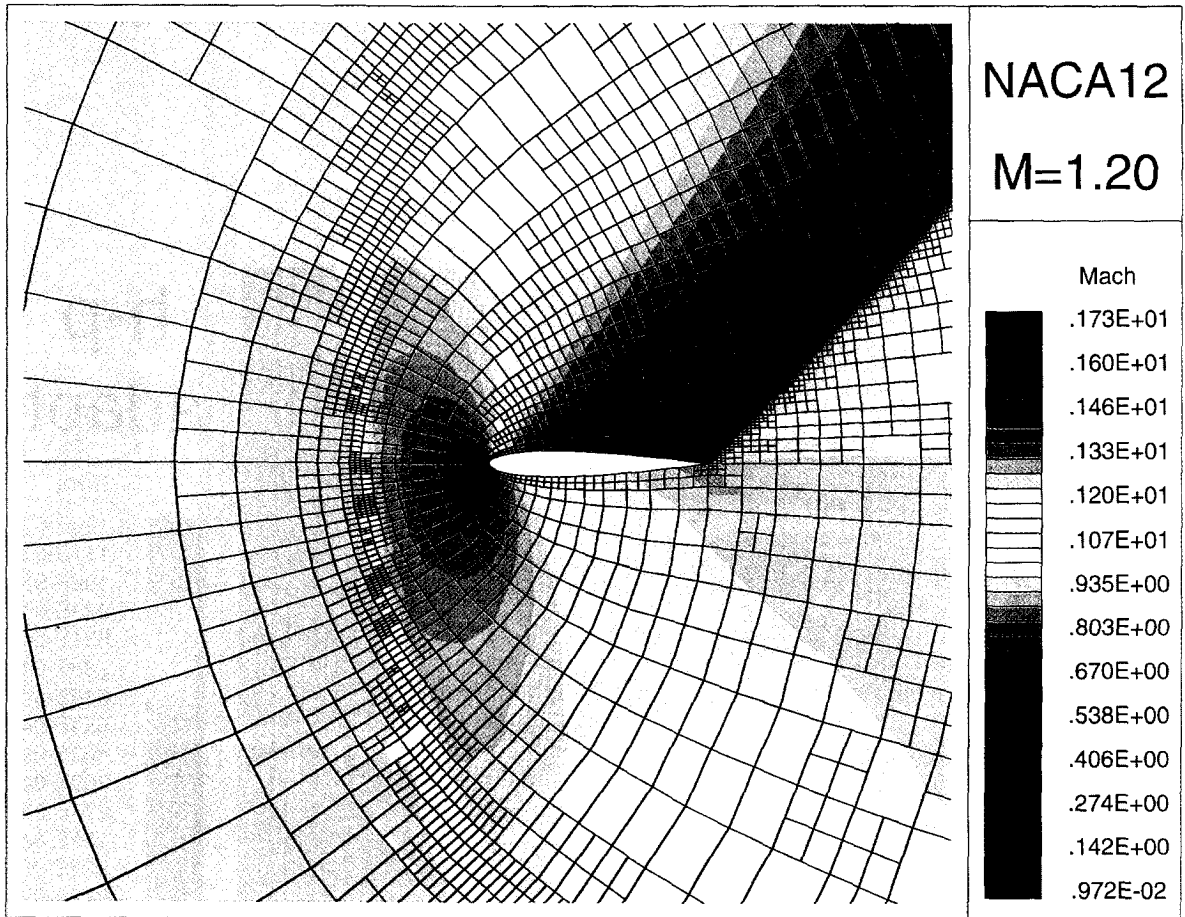

Fig. 27. NACA0012, $M_\infty = 1.20$, incidence 7.0°, mesh and Mach number.

4.2. Extensions to nonlinear systems

The basic approach outlined thus far for convection–diffusion problems can be extended to nonlinear systems of equations with and without diffusion terms. For example, in [10–12] we presented extensions to the Euler and Navier–Stokes equations. Some representative results are shown in Figs. 27–30.

The first set of figures corresponds to the transonic flow around a NACA0012 profile at $M_x = 1.2$ and incidence angle 7.0°. The inviscid Euler equations are used to model this problem. Fig. 27 shows the final mesh after adaptation with the Mach number distribution, and Fig. 28 shows the pressure distribution. These figures show the advantage of using discontinuous approximations even in cases where the shock waves are oblique with respect to the original mesh, note that the oblique shock wave that starts at the trailing edge of the airfoil is very well resolved.

The second set of figures corresponds to a driven cavity problem at Re 7500 as described in [24]. The solution is obtained with a mesh of quadratic elements which is equivalent (in number of degrees of freedom) to a mesh of 60×60 linear elements as that shown in Fig. 29, this figure also shows the pressure distribution on the background. Note that the pressure range shown is considerably narrower than the actual range, which is very wide because of the presence of singularities at the top corners of the cavity. The cutoff values $[p_{min}, p_{max}]$ applied to the range of pressure allow to observe small changes within the domain, excluding the areas adjacent to the top corners. Fig. 30 shows the streamline pattern. Velocity profiles through the middle vertical and horizontal planes are in close agreement with those reported in [24].
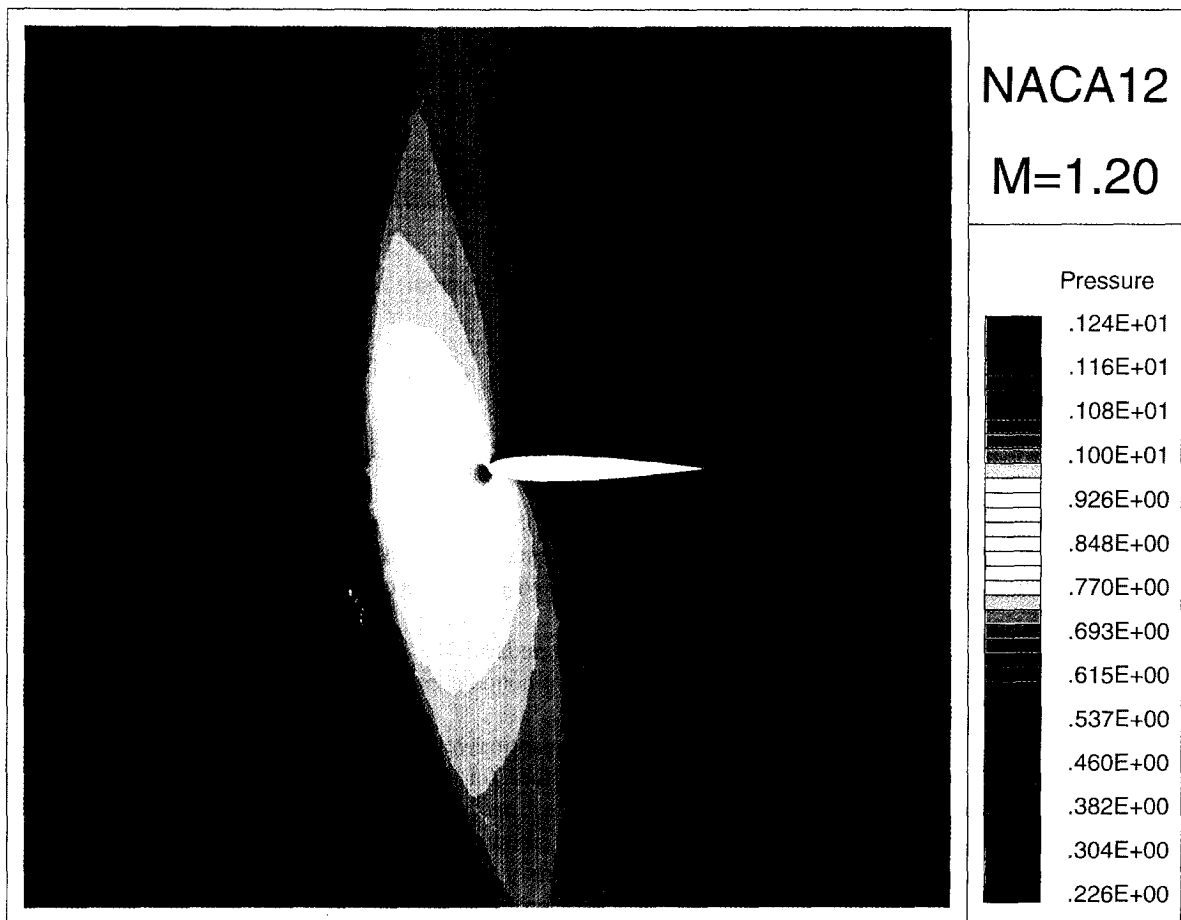

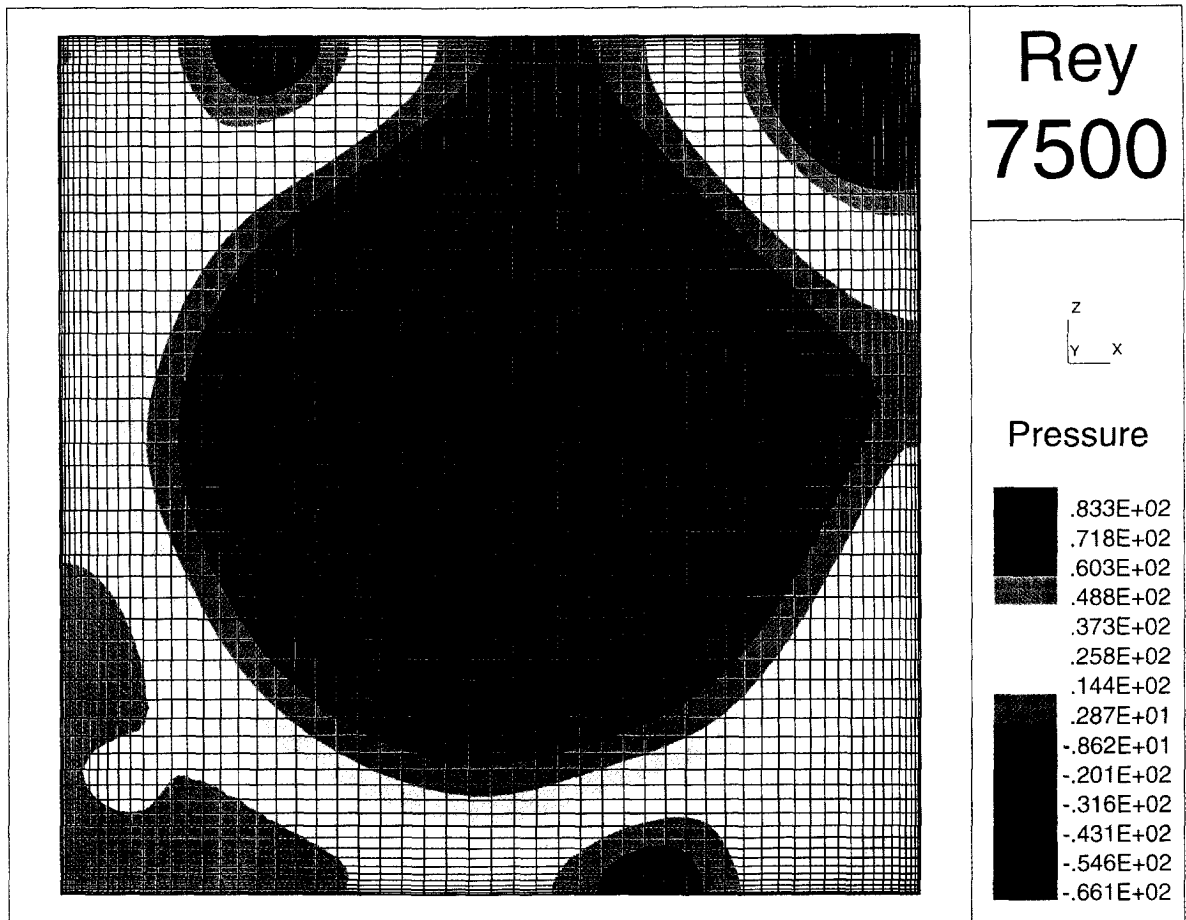Fig. 28. NACA0012, $M_x = 1.20$, incidence 7.0°, pressure.

Fig. 29. Driven cavity at Re = 7500, mesh and pressure contours.

5. Concluding remarks

The salient properties of the discontinuous Galerkin formulation introduced in this paper can be summarized as follows:

- the method is capable of solving convection–diffusion problems with an hp-approximation methodology. If the local regularity of the solution is high the p-approximation can be used and the method delivers very high accuracy; otherwise the h-approximation can be used and the error is reduced by local refinement of the mesh;

- approximate solutions of unresolved flows (e.g. boundary layers) do not suffer from widespread oscillations, for these cases the treatment of interelement boundaries prevents the appearance and spreading of numerical oscillations;

- stability studies and numerical tests demonstrate quantitatively and qualitatively the superiority of discontinuous solutions over continuous Galerkin solutions for convection–diffusion problems;

- discrete representations are stable in the sense that the real part of the eigenvalues associated with the space discretization are strictly negative, a property that allows the use of time marching schemes for time-dependent problems and also allows to solve steady state problems with explicit schemes. Many discontinuous approximations of convection–diffusion problems do not have this property;

- an a priori error estimate for high Pe numbers indicates that the method delivers optimal h-convergence rate (accuracy); and
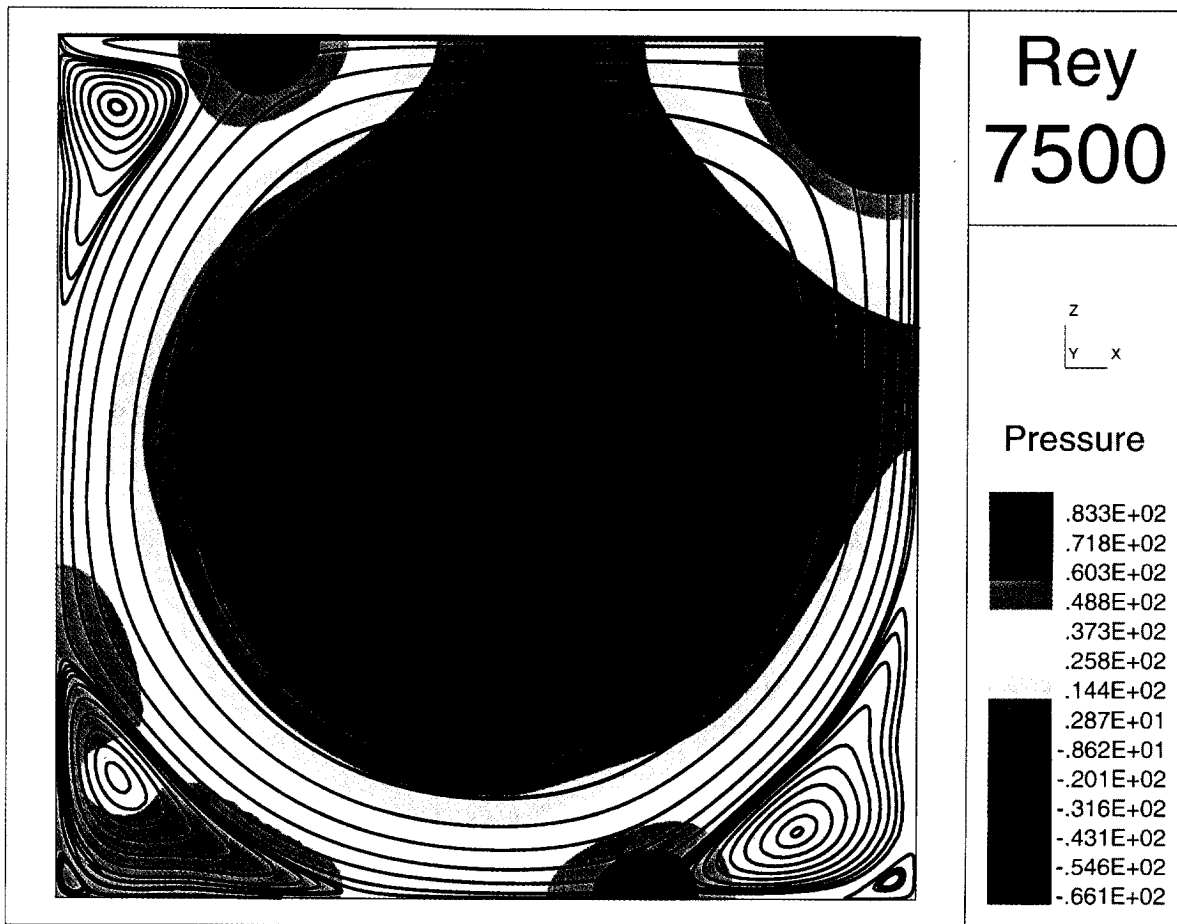
Fig. 30. Driven cavity at Re = 7500, pressure contours and streamlines.

- contrasting other techniques that use artificial diffusion to improve the stability of continuous Galerkin approximations (e.g. SUPG), the present discontinuous Galerkin method does not introduce such mesh-size dependent terms in the governing equations, which allows for approximation with unlimited order of accuracy; namely, the order of accuracy grows linearly with the order of the basis functions p.

Acknowledgment

Appendix A. The discontinuous Galerkin method applied to the convection equation

This appendix includes a summary of the discontinuous Galerkin method applied to linear hyperbolic problems. It includes error estimates and definitions of norms that are used for the analysis of hyperbolic problems [29,27,15]. We have also included a weak formulation which has not been given the importance that it deserves in the literature.

A.1. Review of a model governing equation and the associated finite element formulation

This section describes the *basic* governing equation and Discontinuous Galerkin formulation that have been utilized in the literature to obtain a priori error estimates.

Let Ω be a bounded Lipschitz domain in $\mathbb{R}^d$, such as the polygonal domain in $\mathbb{R}^2$ depicted in Fig. A.1. The governing equation is the following linear scalar hyperbolic conservation law (strong form)

$$\boxed{\begin{aligned} \boldsymbol{\nabla}\cdot(\boldsymbol{\beta}u) + \sigma u &= S && \text{in } \Omega \subset \mathbb{R}^d \\ u &= f && \text{on } \Gamma_- \end{aligned}}$$

(A.1)

where $\boldsymbol{\beta}$ is a *constant unit* velocity vector, $\sigma \in L^\infty\Omega \,|\, \sigma > 0$ a.e. in Ω, $S \in L^2(\Omega)$, $f \in L^2(\Gamma_-)$, $\Gamma_- = \{x \in \partial\Omega \,|\, (\boldsymbol{\beta}\cdot\boldsymbol{n})(x) < 0\}$, $\Gamma_+ = \partial\Omega\backslash\Gamma_-$, and $\boldsymbol{n}$ represents the outward normal to $\partial\Omega$. The assumption of $\boldsymbol{\beta}$ being a *constant unit* vector was used in the literature to obtain a priori error estimates, but in general we do not make this assumption.

A.1.1. Discontinuous Galerkin formulation

The partition of Ω and *all the related nomenclature* are presented in Section 2.1.

Let $V(\mathscr{P}_h)$ be the space of functions

$$V(\mathscr{P}_h) = \{v \in L^2(\Omega) : \boldsymbol{\nabla}\cdot(\boldsymbol{\beta}v)|_{\Omega_e} \in L^2(\Omega_e) \ \forall \ \Omega_e \in \mathscr{P}_h(\Omega)\}\,.$$

(A.2)

The discontinuous Galerkin formulation can be stated as follows:

$$\boxed{\begin{aligned} &\text{Find } u \in V(\mathscr{P}_h) \text{ such that} \\ &\int_{\Omega_e} v(\boldsymbol{\nabla}\cdot(\boldsymbol{\beta}u) + \sigma u - S)\,\mathrm{d}x - \int_{\partial\Omega_e^-\backslash\Gamma_-} v(u^+ - u^-)(\boldsymbol{\beta}\cdot\boldsymbol{n})\,\mathrm{d}s \\ &\quad - \int_{\partial\Omega_e^-\cap\Gamma_-} v(u^+ - f)(\boldsymbol{\beta}\cdot\boldsymbol{n})\,\mathrm{d}s = 0 \\ &\forall\, v \in V(\mathscr{P}_h)\,, \quad \forall\, \Omega_e \in \mathscr{P}_h(\Omega) \end{aligned}}$$

(A.3)

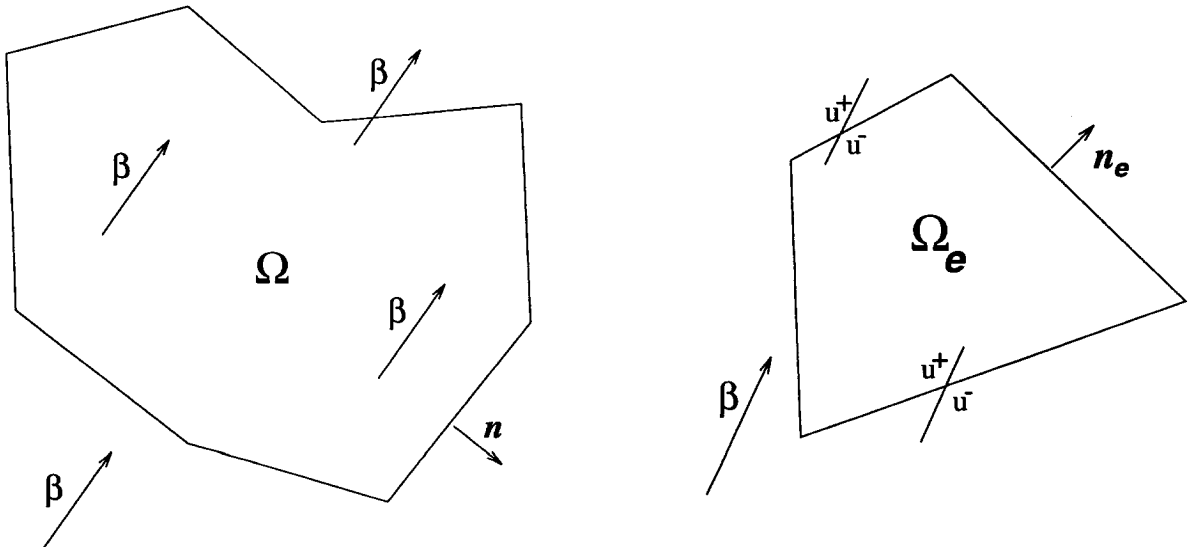
Fig. A.1. Physical problem and symbolic representation of $u^\pm$.

where

$$\partial \Omega_e^- = \{ x \in \partial \Omega_e \mid \boldsymbol{\beta} \cdot \boldsymbol{n}_e(x) < 0 \},$$

$$u^\pm = \lim_{\epsilon \to 0^+} u(x \pm \epsilon \boldsymbol{\beta}), \quad \text{for } \dot{x} \in \Gamma_{\text{int}} = \left(\bigcup_{\Omega_e \in \mathscr{P}_h(\Omega)} \partial \Omega_e \right) \backslash \partial \Omega.$$

A.2. Discontinuous Galerkin approximation

Let $P_{p_e}(\Omega_e)$ be the space of of polynomials ψ on element $\Omega_e \in \mathscr{P}_h(\Omega)$ defined through a transformation $\psi = \hat{\psi} \circ F_{\Omega_e}^{-1}$, where $\hat{\psi}$ are polynomials of degree $\leqslant p_e$ defined on the master element $\hat{\Omega}$, and the transformation F_{Ω_e} is such that $\Omega_e = F_{\Omega_e}(\hat{\Omega})$.

Let us define a finite-dimensional subspace of $V(\mathscr{P}_h)$ as follows:

$$V_p(\mathscr{P}_h) = \{ v \in V(\mathscr{P}_h) : v|_{\Omega_e} \in P_{p_e}(\Omega_e), \forall \Omega_e \in \mathscr{P}_h \}.$$

With $V_p(\mathscr{P}_h)$, the finite element approximation can be stated as follows:

Find $u_h \in V(\mathscr{P}_h)$ such that

$$\int_{\Omega_e} v_h(\boldsymbol{\nabla} \cdot (\boldsymbol{\beta} u_h) + \sigma u_h - S)\, \mathrm{d}x - \int_{\partial \Omega_e^- \backslash \Gamma_-} v(u_h^+ - u_h^-)(\boldsymbol{\beta} \cdot \boldsymbol{n})\, \mathrm{d}s$$

$$- \int_{\partial \Omega_e^- \cap \Gamma_-} v_h(u_h^+ - f)(\boldsymbol{\beta} \cdot \boldsymbol{n})\, \mathrm{d}s = 0$$

$$\forall v_h \in V_p(\mathscr{P}_h), \quad \forall \Omega_e \in \mathscr{P}_h(\Omega)$$

Here, we should note that under the assumption of polygonal subdomains and constant transport velocity, the above system can be solved element by element, in one sweep.

A.3. A priori error estimates

For a regular discretization consisting of triangles and quadrilaterals, Lesaint and Raviart [29] proved the following a priori error estimate in the L^2-norm:

$$\| u_h - u \|_0 \leqslant C h^p \| u \|_{p+1}, \tag{A.4}$$

where

$$h = \max_{\Omega_e \in \mathscr{P}_h(\Omega)} \text{diam}(\Omega_e),$$

and $\| . \|_{p+1}$ represents the classical Sobolev norm for $H^{p+1}(\Omega)$.

Using mesh dependent norms, Johnson and Pitkäranta [27] obtained a sharper estimate

$$\| u_h - u \|_0 \leqslant \| | u_h - u | \|_\beta \leqslant C h^{p+1/2} \| u \|_{p+1},$$

$$\| | v | \|_\beta = \left\{ \sum_{\Omega_e \in \mathscr{P}_h} [h_e \| v_\beta \|_{0,\Omega_e}^2 + \| v \|_{0,\Omega_e}^2 + \langle\!\langle v^+ - v^- \rangle\!\rangle_{\partial \Omega_e \backslash \Gamma_-}^2 + \langle\!\langle v \rangle\!\rangle_{\partial \Omega_e \cap \partial \Omega}^2] \right\}^{1/2} \tag{A.5}$$

where $v_\beta = \boldsymbol{\nabla} v \cdot \boldsymbol{\beta}$, and

$$\langle\!\langle v \rangle\!\rangle_\gamma^2 = \int_\gamma v^2 |\boldsymbol{\beta} \cdot \boldsymbol{n}| \, \mathrm{d}s \, , \quad \gamma \subset \partial\Omega_e \, .$$

For the case in which all elements are rectangles, Lesaint and Raviart [29] proved the following error estimate

$$\|u_h - u\|_0 \leqslant C h^{p+1} \|u\|_{p+2} \tag{A.6}$$

and for the case in which all elements are triangles, Richter [40] proved (A.6) assuming uniformity in the triangulation.

Bey and Oden [15] proved the following h-p a priori error estimate

$$\||u_h - u|\|_{hp,\beta} \leqslant C \left\{ \sum_{\Omega_e \in \mathscr{P}_h} \left(\frac{h_e^{2p_e+1}}{p_e^{2p_e}} \|u\|_{p_e+1,\Omega_e}^2 \right) \right\}^{1/2} \tag{A.7}$$

where

$$\||v|\|_{hp,\beta} = \left\{ \sum_{\Omega_e \in \mathscr{P}_h} \left[\frac{h_e}{p_e^2} \|v_\beta\|_{0,\Omega_e}^2 + \|v\|_{0,\Omega_e}^2 + \langle\!\langle v^+ - v^- \rangle\!\rangle_{\partial\Omega_e \backslash \Gamma_-}^2 + \langle\!\langle v \rangle\!\rangle_{\partial\Omega_e \cap \partial\Omega}^2 \right] \right\}^{1/2} ,$$

the previous estimate is valid if every element in the partition has order $p_e \geqslant 1$.

A.4. Alternative discontinuous Galerkin formulation

In general, when the velocity field $\boldsymbol{\beta}$ is a function of $\boldsymbol{x}$, and/or the partition $\mathscr{P}_h(\Omega)$ contains elements with curved boundaries, the finite element formulation will not be uncoupled and the element by element technique can not be applied. It is convenient to utilize the following conservative formulation obtained when the divergence term is integrated by parts:

Find $u \in V(\mathscr{P}_h)$ such that

$$\int_{\Omega_e} [-(\nabla v \cdot \boldsymbol{\beta})u + v(\sigma u - S)] \, \mathrm{d}x + \int_{\partial\Omega_e \backslash \Gamma_-} v u^- (\boldsymbol{\beta} \cdot \boldsymbol{n}_e) \, \mathrm{d}s$$

$$+ \int_{\partial\Omega_e \cap \Gamma_-} v f (\boldsymbol{\beta} \cdot \boldsymbol{n}_e) \, \mathrm{d}s = 0 \, , \quad \forall v \in V(\mathscr{P}_h) \, , \quad \forall \Omega_e \in \mathscr{P}_h(\Omega)$$

---

which can also be solved element by element in one sweep when the transport velocity is a constant vector and the elements are polygons, otherwise it is a coupled system of equations and has to be solved as such.

References

[1] S.R. Allmaras, A coupled Euler/navier–Stokes algorithm for 2-D unsteady transonic shock/boundary-layer interaction, Ph.D. Dissertation, Massachusetts Institute of Technology, Feb. 1989.

[2] T. Arbogast and M.F. Wheeler, A characteristic-mixed finite element method for convection-dominated transport problems, SIAM J. Numer. Anal. 32 (1995) 404–424.

[3] D.N. Arnold, An interior penalty finite element method with discontinuous elements, SIAM J. Numer. Anal. 19(4) (1982) 742–760.

[4] H.L. Atkins and C.-W. Shu, Quadrature-free implementation of discontinuous Galerkin methods for hyperbolic equations, ICASE Report 96-51, 1996.

[5] A.K. Aziz and I. Babuška, The Mathematical Foundations of the Finite Element Method with Applications to Partial Differential Equations (Academic Press, 1972).

[6] I. Babuška and M. Suri, The hp-version of the finite element method with quasiuniform meshes, Math. Model. Numer. Anal. 21 (1987) 199–238.

[7] I. Babuška, J. Tinsley Oden and C.E. Baumann, A discontinuous hp finite element method for diffusion problems: 1-D Analysis, Comput. Math. Applic., also TICAM Report 97-22, to appear.

[8] F. Bassi and R. Rebay, A high-order accurate discontinuous finite element method for the numerical solution of the compressible Navier–Stokes equations, J. Comput. Phys., submitted.

[9] F. Bassi, R. Rebay, M. Savini and S. Pedinotti, The Discontinuous Galerkin method applied to CFD problems, in: Second European Conf. on Turbomachinery, Fluid Dynamics and Thermodynamics, ASME, 1995.

[10] C.E. Baumann, An hp-adaptive discontinuous finite element method for computational fluid dynamics, Ph.D. Dissertation, The University of Texas at Austin, Aug. 1997.

[11] C.E. Baumann and J. Tinsley Oden, A discontinuous hp finite element method for the solution of the Euler equations of Gas Dynamics, in: Tenth Int. Conf. on Finite Elements in Fluids, Jan. 5–8, 1998.

[12] C.E. Baumann and J. Tinsley Oden, A discontinuous hp finite element method for the solution of the Navier–Stokes equations, in: Tenth Int. Conf. on Finite Elements in Fluids, Jan. 5–8, 1998.

[13] K.S. Bey and J.T. Oden, A Runge–Kutta discontinuous finite element method for high speed flows, in: AIAA 10th Computational Fluid Dynamics Conference, June 1991.

[14] K.S. Bey, J.T. Oden and A. Patra, hp-Version discontinuous Galerkin methods for hyperbolic conservation laws, Comput. Methods Appl. Mech. Engrg. 133(3-4) (1996) 259–286.

[15] K. S. Bey, An hp-adaptive discontinuous Galerkin method for hyperbolic conservation laws, Ph.D. dissertation, The University of Texas at Austin, May 1994.

[16] B. Cockburn, An introduction to the discontinuous Galerkin method for convection-dominated problems, School of Mathematics, University of Minnesota, 1997.

[17] B. Cockburn, S. Hou and C.W. Shu, TVB Runge–Kutta local projection discontinuous Galerkin finite element for conservation laws IV: The multi-dimensional case, Math. Comput. 54 (1990) 545.

[18] B. Cockburn, S. Hou and C.W. Shu, The Runge–Kutta discontinuous Galerkin method for conservation laws V: Multidimensional systems, ICASE Report 97-43, 1997.

[19] B. Cockburn, S.Y. Lin and C.W. Shu, TVB Runge–Kutta local projection discontinuous Galerkin finite element for conservation laws III: One-dimensional systems, J. Comput. Phys. 84 (1989) 90–113.

[20] B. Cockburn and C.W. Shu, TVB Runge–Kutta local projection discontinuous Galerkin finite element for conservation laws II: General framework, Math. Comput. 52 (1989) 411–435.

[21] B. Cockburn and C.W. Shu, The local discontinuous Galerkin method for time dependent convection–diffusion systems, SIAM J. Numer. Anal., submitted.

[22] C.N. Dawson, Godunov-mixed methods for advection–diffusion equations, SIAM J. Numer. Anal. 30 (1993) 1315–1332.

[23] L.M. Delves and C. A. Hall, An implicit matching principle for global element calculations, J. Inst. Math. Appl. 23 (1979) 223–234.

[24] U. Ghia, K.N. Ghia and C.T. Shin, High-Re solutions for incompressible flow using the Navier–Stokes equations and a multigrid method, J. Comput. Phys. 48 (1982) 387–411.

[25] J.A. Hendry and L.M. Delves, The global element method applied to a harmonic mixed boundary value problem, J. Comput. Phys. 33 (1979) 33–44.

[26] C. Hu and C.-W. Shu, A discontinuous Galerkin finite element method for the Hamilton–Jacobi equations, Division of Applied Mathematics, Brown University, 1997.

[27] C. Johnson and J.Pitkäranta, An analysis of the discontinuous Galerkin method for a scalar hyperbolic equation, Math. Comput. 46 (1986) 1–26.

[28] J. Lang and A. Walter, An adaptive discontinuous finite element method for the transport equation, J. Comput. Phys. 117 (1995) 28–34.

[29] P. Lesaint and P.A. Raviart, On a finite element method for solving the neutron transport, in: C. de Boor, ed., Mathematical Aspects of Finite Elements in Partial Differential Equations (Academic Press, 1974) 89–123.

[30] P. Lesaint and P.A. Raviart, Finite element collocation methods for first-order systems, Math. Comput. 33(147) (1979) 891–918.

[31] I. Lomtev and G.E. Karniadakis, A discontinuous Galerkin method for the Navier–Stokes equations, Int. J. Numer. Methods Fluids, submitted.

[32] I. Lomtev and G.E. Karniadakis, Simulations of viscous supersonic flows on unstructured meshes, AIAA-97-0754, 1997.

[33] I. Lomtev, C.B. Quillen and G.E. Karniadakis, Spectral/hp methods for viscous compressible flows on unstructured 2d meshes, J. Comput. Phys. (1998) to appear.

[34] I. Lomtev, C.W. Quillen and G. Karniadakis, Spectral/hp methods for viscous compressible flows on unstructured 2d meshes, Technical report, Center for Fluid Mechanics Turbulence and Computation, Brown University, Box 1966, Providence RI 02912, Dec. 1996.

[35] R.B. Lowrie, Compact higher-order numerical methods for hyperbolic conservation laws, Ph.D. Dissertation, University of Michigan, 1996.

[36] J. Nitsche, Über ein Variationsprinzip zur Lösung von Dirichlet Problemen bei Verwendung von Teilräumen, die keinen Randbedingungen unterworfen sind, Abh. Math. Sem. Univ. Hamburg 36 (1971) 9–15.

[37] J.T. Oden and G.F. Carey, Texas Finite Elements Series, Vol. IV—Mathematical Aspects (Prentice-Hall, 1983).

[38] J. Tinsley Oden, I. Babuška and C.E. Baumann, A discontinuous hp finite element method for diffusion problems, J. Comput. Phys., also TICAM Report 97-21, to appear.

[39] P. Percell and M.F. Wheeler, A local residual finite element procedure for elliptic equations, SIAM J. Numer. Anal. 15(4) (1978) 705–714.

[40] G.R. Richter, An optimal-order error estimate for the discontinuous Galerkin method, Math. Comput. 50 (1988) 75–88.

[41] T.C. Warburton, I. Lomtev, R.M. Kirby and G.E. Karniadakis, A discontinuous Galerkin method for the Navier–Stokes equations on hybrid grids, Center for Fluid Mechanics 97-14, Division of Applied Mathematics, Brown University, 1997.